

RECEIVED: March 18, 2022

REVISED: May 10, 2022

ACCEPTED: May 23, 2022

PUBLISHED: June 21, 2022

Interactions of strings on a T-fold

Yuji Satoh and Yuji Sugawara

Department of Applied Physics, University of Fukui

Bunkyo 3-9-1, Fukui 910-8507, Japan

Department of Physical Sciences, College of Science and Engineering

Ritsumeikan University, Shiga 525-8577, Japan

E-mail: ysatoh@u-fukui.ac.jp, ysugawa@se.ritsumei.ac.jp

ABSTRACT: We consider the interactions of strings on T-folds from the world-sheet point of view which are exact in α' . As a concrete example, we take a model where the internal torus at the SO(8) enhancement point is twisted by T-duality (T-folded), and compute the scattering amplitudes of a class of massless strings. The four-point amplitudes involving both twisted and untwisted strings are obtained in a closed form in terms of the hypergeometric function. By their factorization, the three-point coupling of the twisted and untwisted strings is found to be suppressed by the chiral momenta along the internal torus, and quantized in integer powers of $1/4$. The asymptotic forms of the four-point amplitudes in high-energy limits are also obtained. Our results rely only on general properties of the asymmetric orbifold by the T-duality twist and of the Lie algebra lattice from the symmetry enhancement, and thus may be extended qualitatively to more general T-folds.

KEYWORDS: Conformal Field Models in String Theory, String Duality, Superstrings and Heterotic Strings

ARXIV EPRINT: [2203.05841](https://arxiv.org/abs/2203.05841)

Contents

1	Introduction	1
2	A model of strings on T-folds	3
2.1	T-fold from SO(8) torus	3
2.2	Partition function and spectrum	5
3	Vertex operators	6
3.1	Classification of spectrum by conjugacy classes	6
3.2	Massless strings in the untwisted sector	7
3.3	Massless strings in the twisted sector	8
4	Amplitudes with vanishing right-moving internal momenta	10
4.1	Three-point amplitudes involving the twisted sector	10
4.2	Four-point amplitudes	11
5	Amplitudes with non-vanishing right-moving internal momenta	14
5.1	Three-point amplitudes	14
5.2	Four-point amplitudes	15
5.3	Poles of the amplitudes	16
5.4	Suppression of the three-point coupling	17
5.5	High energy behaviors	18
6	Discussion	22
7	Components of partition function	24
8	Twist fields for a chiral boson	25
9	Formulas of integrals	26
10	SO(4) gamma matrices	29

1 Introduction

Strings can propagate in backgrounds which are not geometric in the conventional sense. Although each appropriate conformal field theory (CFT) on the world-sheet gives a string vacuum, its target-space interpretation is not always obvious. It is also possible to think of the backgrounds where the transition functions for the target space involve the symmetries intrinsic to string theory, namely, the string dualities. In the case of T-duality, the corresponding “(non-)geometry” is named the T-fold [1–4]. These non-geometric backgrounds

are relevant in understanding the string vacua. Furthermore, those involving the string dualities would provide clues in understanding the dualities and the new formulations of string theory, such as Double Field Theory (DFT) [5], in which the dualities are manifest.

Among non-geometric backgrounds in string theory, we focus on the T-fold in this paper. At low-energy, strings on T-folds can be analyzed by supergravity, or under certain consistent truncation including the winding modes, by DFT. Moreover, in order to study them in the regime where their quantum effects are further incorporated, their formulation based on the world-sheet CFT would be necessary. Since the T-folding is realized on the world-sheet by gauging a twist involving T-duality which acts asymmetrically on the left- and the right-mover, T-folds are described by a particular class of asymmetric orbifold CFTs.¹

In such a formulation, it has been known that one encounters a seeming puzzle [9–12]: to be concrete, let us consider the T-duality transformation which is realized by a chiral reflection of the coordinate fields e.g. in the right-mover, and hence acts as a \mathbb{Z}_2 transformation. The modular transformation of the world-sheet partition functions, however, generally forms a $\mathbb{Z}_{n>2}$ representation due to the non-trivial phases in the twisted sectors which remain as a consequence of the left-right asymmetry. A resolution to this puzzle is to note that the \mathbb{Z}_2 action in the target space may be lifted to more general actions on the world-sheet [9, 13–15]. In other words, T-duality may have a different representation there, similarly to the spin representation for the orthogonal group.

Once the puzzle is cleared, it is conceptually straightforward to advance the studies of strings on T-folds by the world-sheet theories, though it is still non-trivial in practice since the construction and the analysis of the corresponding asymmetric orbifold theories are rather involved. In this respect, a class of the asymmetric orbifold CFTs describing T-folds, or their modular invariant partition functions, has been constructed in a systematic manner by making use of Lie algebra lattices [13, 14]. Motivated by the cosmological constant problem as in [13], related asymmetric orbifold models have been constructed [16–18]. An application of these CFTs/models to that problem has been discussed [19].

The purpose of this paper is to make a step toward the studies of strings on T-folds in depth which are exact in α' beyond the regime of supergravity and DFT. In particular, we take a supersymmetric model constructed in [13] as a concrete example, where the internal torus at the SO(8) enhancement point is twisted by T-duality (T-folded), and study the interactions of the strings. Our prime interest is to figure out what happens when the strings twisted by T-duality, which might be rather exotic from the conventional point of view, interact with the untwisted strings. As simple examples to this end, we consider a class of ten-dimensional massless strings, which are excited by the internal momenta above the four-dimensional massless strings in the untwisted sector or those in the ground states in the twisted sector. We first construct their vertex operators. The T-duality twist, or the chiral reflection in this case, is implemented by the twist fields of the type in the Ashkin-Teller model [20–27] for the bosonic coordinate fields and by the spin fields for the world-sheet fermions.

¹For the world-sheet doubled formalism, see [4, 6, 7]. For a review on non-geometric backgrounds in string theory in general, see e.g. [8].

We then compute their three- and four-point amplitudes, focusing on the NS-NS sector. The four-point amplitudes involving two twisted and two untwisted strings are obtained in a closed form in terms of the hypergeometric function. By their factorization, we find that the three-point amplitudes among the twisted and untwisted strings are suppressed by the momenta flowing along the T-folded internal torus. Its mechanism is essentially the same as that for general symmetric orbifolds discussed in [28]. In our case of an asymmetric orbifold based on a Lie algebra lattice, only the momenta in the right-mover contribute to the suppression. In addition, the three-point coupling is quantized in integer powers of N^{-2} with $N = 2$, where N comes from $\mathbb{Z}_{N=2}$ of the T-duality twist (in the untwisted sector) and the exponent 2 from the length of the roots of $SO(8)$. This result of the suppression includes stringy effects through the winding modes which are non-perturbative from the sigma-model point of view.

We also consider high-energy limits of the amplitudes, which correspond to $\alpha' \rightarrow \infty$ opposite to the particle limit $\alpha' \rightarrow 0$. In a hard-scattering limit where (the absolute values of) all the Mandelstam variables become large, the angle dependence for the momenta along the twisted internal torus takes the same form as that for the external momenta in the usual hard-scattering. The sign of its exponent given by the magnitude of the incident momenta is, however, opposite. We find that both of the two saddle points of the integrand of the amplitude are dominant, and each gives the correct result in the hard-scattering limit up to a momentum dependent phase.

Although we work with a concrete model of strings on T-folds, our analyses rely only on general properties of the asymmetric orbifold by the T-duality twist and of the Lie algebra lattice associated with the twisted internal torus. Thus, our results may be extended qualitatively to more general T-folds.

The rest of this paper is organized as follows. In section 2, we review a model constructed in [13], which is used in this paper, and summarize its properties. This section sets up our notation. In section 3, we classify the spectrum of the model, and construct the vertex operators of the strings mentioned above. In section 4, we compute their three- and four-point amplitudes in the case of the vanishing right-moving momenta along the T-duality twisted torus. This section serves as a preparation for the next section, and provides a check of the results there as well. In section 5, we compute the amplitudes in the general case with the non-vanishing right-moving momenta along the twisted torus. We analyze their properties including the suppression of the coupling and the high-energy behaviors. We conclude with a summary and discussion in section 6. In the appendix, we summarize our conventions, some formulas and details of our computations, which are used in the main text.

2 A model of strings on T-folds

2.1 T-fold from $SO(8)$ torus

As a concrete example, we consider a model of strings on T-folds which is constructed in [13]. This model is obtained by gauging a twist of $\mathcal{M} = \mathbb{R}^{1,3} \times S^1 \times \mathbb{R}_{\text{base}} \times T_{\text{fiber}}^4$ which involves T-duality, where T_{fiber}^4 is the torus at the $SO(8)$ enhancement point of the moduli.

We denote the coordinate fields by X^M ($M = 0, 1, \dots, 9$). For later use, we introduce the indices for each part of \mathcal{M} ; for example, $\tilde{\mu} = M = 0, \dots, 3$ for $\mathbb{R}^{1,3}$, $p = M = 4, 5$ for S^1 and \mathbb{R}_{base} respectively, and $a = M = 6, \dots, 9$ for T_{fiber}^4 . The part other than T_{fiber}^4 is also denoted, e.g. by $\mu = M = 0, \dots, 5$. In the untwisted sector, the twist σ for our T-fold is implemented by the T-duality twist or the chiral reflection on T_{fiber}^4 ,

$$(X_L^a, X_R^a) \mapsto (X_L^a, -X_R^a) \quad (a = 6, 7, 8, 9), \quad (2.1)$$

together with the translation in \mathbb{R}_{base} ,

$$X^5 \mapsto X^5 + 2\pi R_5, \quad (2.2)$$

where we have split X^a into the left- and the right-mover as $X^a(z, \bar{z}) = X_L^a(z) + X_R^a(\bar{z})$. Thus, a string wrapped around the base circle along \mathbb{R}_{base} modded out by (2.2) undergoes monodromy due to (2.1) in the fiber torus part T_{fiber}^4 , which characterizes the T-fold. It turns out, as in (2.11) below, that half-integer modes, in addition to integer ones, appear in the spectrum of the momentum along the base circle.²

These $X_{L/R}^a$ are expanded as

$$X_L^a = e_j^a x_L^j - i \frac{\alpha'}{2} p_L^a \ln z + \dots, \quad X_R^a = e_j^a x_R^j - i \frac{\alpha'}{2} p_R^a \ln \bar{z} + \dots, \quad (2.3)$$

with

$$p_L^a = \sqrt{\frac{2}{\alpha'}} e_a^{*j} [n_j + (G - B)_{jk} w^k], \quad p_R^a = \sqrt{\frac{2}{\alpha'}} e_a^{*j} [n_j - (G + B)_{jk} w^k], \quad (2.4)$$

and $n_j, w^j \in \mathbb{Z}$. Here, e_j^a and e_a^{*j} are the vielbein and its inverse, which satisfy

$$e_j^a e_k^a = 2G_{jk}, \quad e_a^{*j} e_a^{*k} = \frac{1}{2} G^{jk}, \quad e_j^a e_b^{*j} = \delta_b^a. \quad (2.5)$$

In the present case, the constant space-time metric G_{ij} and the anti-symmetric tensor B_{ij} are given by the Cartan matrix C_{ij} of $\text{SO}(8)$ as $G_{ij} = \frac{1}{2} C_{ij}$ for any i, j and $B_{ij} = \frac{1}{2} C_{ij}$ for $i > j$. G^{ij} is the inverse of G_{ij} . Thus, e_j^a and e_a^{*j} form the root and the weight lattice of $\text{SO}(8)$, respectively. This also implies that the momenta $\sqrt{\alpha'/2} p_{L/R}^a$ take their value on the $\text{SO}(8)$ lattice. The left- and right-momenta belong to the same conjugacy class, since their difference is given by the root lattice, $\sqrt{\alpha'/2} (p_L^a - p_R^a) = e_j^a w^j$. We follow the notation in [14, 29] for the Lie algebra lattice. The periodicity of $\hat{X}^j := e_a^{*j} X^a \sim \hat{X}^j + \sqrt{\alpha'/2} \times 2\pi m^j$ with $m^j \in \mathbb{Z}$ is translated into $X^a \sim X^a + \sqrt{\alpha'/2} \times 2\pi e_j^a m^j$. The chiral bosons $X_{L/R}^M$ have the standard operator product expansions (OPEs), $X_L^M(z) X_L^N(0) \sim -(\alpha'/2) \eta^{MN} \ln z$ and $X_R^M(\bar{z}) X_R^N(0) \sim -(\alpha'/2) \eta^{MN} \ln \bar{z}$ with $\eta^{MN} = \text{diag}(-1, +1, \dots, +1)$.

For the world-sheet superconformal symmetry to be preserved, the T-duality twist acts also as the chiral reflection on the world-sheet fermions in the untwisted Neveu-Schwarz (NS) sector,

$$(\psi_L^a, \psi_R^a) \mapsto (\psi_L^a, -\psi_R^a) \quad (a = 6, 7, 8, 9). \quad (2.6)$$

²One may start with a base circle with radius $2R_5$ as in [3, 11, 12] instead of \mathbb{R}_{base} , and then consider the T-duality twist accompanied with the half-shift $X^5 \mapsto X^5 + 2\pi R_5$. This is equivalent to the present formulation and leads to the same partition function as in (2.11).

The fermions in the left- and the right-mover, $\psi_L^M(z)$, $\psi_R^M(\bar{z})$, have the OPEs, $\psi_L^M(z)\psi_L^N(0) \sim \eta^{MN}z^{-1}$ and $\psi_R^M(\bar{z})\psi_R^N(0) \sim \eta^{MN}\bar{z}^{-1}$. The action (2.6) determines the T-duality twist in this sector. That in the untwisted Ramond sector is, however, not unique and there are essentially two cases, as understood e.g. through bosonization. When one adopts a bosonization of the right-moving transverse fermions ψ_R^M ,³

$$\begin{aligned} \psi_R^2 \pm i\psi_R^3 &=: \sqrt{2}e^{\pm iH_R^1}, & \psi_R^4 \pm i\psi_R^5 &=: \sqrt{2}e^{\pm iH_R^2}, \\ \psi_R^6 \pm i\psi_R^7 &=: \sqrt{2}e^{\pm iH_R^3}, & \psi_R^8 \pm i\psi_R^9 &=: \sqrt{2}e^{\pm iH_R^4}, \end{aligned} \tag{2.7}$$

by the free bosons $H_R^k(\bar{z})$ with $H_R^k(\bar{z})H_R^l(0) \sim -\delta^{kl} \ln \bar{z}$, the action (2.6) is translated into

$$\left(H_R^1, H_R^2, H_R^3, H_R^4\right) \longmapsto \left(H_R^1, H_R^2, H_R^3 + \pi, H_R^4 - \pi\right). \tag{2.8}$$

In terms of these H_R^k , the spin fields are given by

$$S_R(\epsilon) = \check{S}_R \hat{S}_R, \quad \check{S}_R := e^{\frac{i}{2} \sum_{k=1}^2 \epsilon_k H_R^k}, \quad \hat{S}_R := e^{\frac{i}{2} \sum_{k=3}^4 \epsilon_k H_R^k}, \tag{2.9}$$

with $\epsilon_k = \pm 1$. We denote the spin fields also by using the spinor indices e.g. as S_R^α instead of $S_R(\epsilon)$. Then, the T-duality twist squares to the identity, and thus the twist becomes \mathbb{Z}_2 also in this sector.

Alternatively, one can bosonize ψ_R^M so that two of ψ_R^a ($a = 6, \dots, 9$) for T_{fiber}^4 are mixed with those for the other part ψ_R^M ($M = 2, \dots, 5$). In this case, (2.6) results in a \mathbb{Z}_4 action in the untwisted Ramond sector. In the following, we consider the first case in (2.7), (2.8).

2.2 Partition function and spectrum

The actions (2.1), (2.2), (2.6), (2.8) determine the twist σ for the T-fold in the untwisted sector. Together with the Gliozzi-Scherk-Olive (GSO) projected untwisted partition function, they also determine the partition function twisted once by σ . Those in the twisted sectors are obtained from them by modular transformations. Consequently, the partition function for the transverse part becomes

$$\begin{aligned} Z(\tau, \bar{\tau}) &= Z_{\mathbb{R}^{1,3} \times S^1}^{\text{tr}}(\tau, \bar{\tau}) \mathcal{J}(\tau) Z_{\text{tw}}(\tau, \bar{\tau}), \\ Z_{\text{tw}}(\tau, \bar{\tau}) &= \sum_{w,m \in \mathbb{Z}} Z_{(w,m)}^{\text{base}}(\tau, \bar{\tau}) F_{(w,m)}^{T^4}(\tau, \bar{\tau}) \overline{f_{(w,m)}(\tau)}. \end{aligned} \tag{2.10}$$

Here, τ is the modulus of the world-sheet torus. $Z_{\mathbb{R}^{1,3} \times S^1}^{\text{tr}}$, $Z_{(w,m)}^{\text{base}}$, $F_{(w,m)}^{T^4}$ are the partition functions from X^μ ($\mu = 2, 3, 4$) for the transverse part of $\mathbb{R}^{1,3} \times S^1$, from X^5 for \mathbb{R}_{base} , and from X^a ($a = 6, \dots, 9$) for T_{fiber}^4 , respectively. \mathcal{J} comes from the left-moving fermions ψ_L^M ($M = 2, \dots, 9$), whereas $\overline{f_{(w,m)}}$ from the right-moving fermions ψ_R^M ($M = 2, \dots, 9$). The explicit form of $Z_{\mathbb{R}^{1,3} \times S^1}^{\text{tr}}$ is the standard one, which we omit. Those for the other components are listed in appendix 7.

We note that the action of the T-duality twist on the world-sheet is generally uplifted [9, 13–15]. In the present case, it becomes \mathbb{Z}_4 on the internal T_{fiber}^4 part as in (7.3) and (7.4)

³We have omitted the cocycles to ensure the anti-commutativity among different fermions.

due to the phases depending on w and m , though it remains \mathbb{Z}_2 in the untwisted sector, i.e. the sector with $w = 0$. The action in the twisted sectors, i.e. the sectors with $w \neq 0$, is found from the expression of the partition function.

This model preserves 24 space-time supercharges (3/4 supersymmetry), 16 of which come from the left-mover and 8 of which from the right-mover. Its spectrum is read off by the Poisson resummation with respect to the temporal winding m , which converts m to the momentum n along $X^5 \in S^1$. After some algebra, one finds

$$Z_{\text{tw}}(\tau, \bar{\tau}) = \frac{1}{|\eta(\tau)|^2} \sum_{w,n \in \mathbb{Z}} q^{\frac{\alpha'}{4} \left(\frac{n}{2R_5} + \frac{R_5}{\alpha'} w \right)^2} \bar{q}^{\frac{\alpha'}{4} \left(\frac{n}{2R_5} - \frac{R_5}{\alpha'} w \right)^2} \sum_{m \in \mathbb{Z}_2} (-1)^{nm} F_{(w,m)}^{T^4}(\tau, \bar{\tau}) \overline{f_{(w,m)}(\tau)}, \tag{2.11}$$

where $q = e^{2\pi i \tau}$ and $\eta(\tau)$ is the Dedekind η function. The spectrum is tachyon-free and maintains the unitarity. Once the phases in $F_{(w,m)}^{T^4}$ and $\overline{f_{(w,m)}}$ are combined and cancelled with each other, the action of the T-duality twist on the product $F_{(w,m)}^{T^4} \overline{f_{(w,m)}}$ becomes \mathbb{Z}_2 in our case. In general, the T-duality twist on the internal part, however, remains to be \mathbb{Z}_k with $k > 2$. In the target space, T-folds generally have non-geometric fluxes (Q -fluxes) [30]. Those in this model may be read off by following a general procedure given in [31] which realizes non-geometric fluxes in terms of world-sheet variables.

3 Vertex operators

3.1 Classification of spectrum by conjugacy classes

The spectrum in the above partition function can be classified by the conjugacy classes of the $SO(2k)$ lattice. We denote by o, v, s, c the conjugacy class including the vacuum, the vector, the spinor and the conjugate-spinor representation, respectively. The characters of $o+v, o-v, s+c, s-c$ are represented by the theta functions $\theta_3^k, \theta_4^k, \theta_2^k, \vartheta_1^k := (-i\theta_1)^k$ divided by η^k .

In the left-mover, $\mathcal{J}(\tau)$ contains v and s of $SO(8)$. In the right-mover, the contents of $f_{(w,m)}$ read

$$\begin{aligned} f_{(0,0)} &: (ov + vo) - (ss + cc), & f_{(0,1)} &: (-ov + vo) - (ss - cc), \\ f_{(1,0)} &: (os + vc) - (sv + co), & f_{(1,1)} &: (os - vc) - (-sv + co). \end{aligned} \tag{3.1}$$

2 Here, we have decomposed the conjugacy classes of $SO(8)$ to those of $SO(4)$ for ψ_R^μ ($\mu = 2, \dots, 5$) and those of $SO(4)$ for ψ_R^a ($a = 6, \dots, 9$), and denoted them from the left to the right. For example, ov means o for ψ_R^μ and v for ψ_R^a .

As a consequence of the $SO(8)$ symmetry in the untwisted sector, $F_{(w,m)}^{T^4}$ are also given by the theta functions as in (7.3), and accordingly decomposed by the conjugacy classes as

$$\begin{aligned} F_{(0,0)}^{T^4} &: o(\overline{oo + vv}) + v(\overline{ov + vo}) + s(\overline{ss + cc}) + c(\overline{sc + cs}), \\ F_{(0,1)}^{T^4} &: o(\overline{oo - vv}) + v(\overline{-ov + vo}) + s(\overline{ss - cc}) + c(\overline{-sc + cs}), \\ F_{(1,0)}^{T^4} &: o(\overline{oc + vs}) + v(\overline{os + vc}) + s(\overline{sv + co}) + c(\overline{so + cv}), \\ F_{(1,1)}^{T^4} &: o(\overline{oc - vs}) + v(\overline{-os + vc}) + s(\overline{sv - co}) + c(\overline{-so + cv}). \end{aligned} \tag{3.2}$$

Here, the left-moving part is represented by the conjugacy classes of $SO(8)$, whereas the right-moving part is represented by those of $SO(4) \oplus SO(4)$ and denoted with the overline $(\overline{\quad})$. While the action of the twist on the untwisted sector directly follows from its definition, the one on the twisted sector is determined uniquely by the modular invariance of the total partition function and the modular covariance of its building blocks. The actions of the twist in the twisted and untwisted sectors are generally different as above.

3.2 Massless strings in the untwisted sector

In $F_{(0,m)}^{T^4}$ for the untwisted sector, the conjugacy classes are specified by the momenta p_L and p_R along T_{fiber}^4 . Under the twist σ for the T-fold, the states may have minus signs from the excitations of the oscillators $\tilde{\alpha}_{-k}^a$ ($k \in \mathbb{Z}_{>0}$) of X_R^a , the odd combination of their oscillator vacua $|p_R\rangle - | - p_R\rangle$, and/or the momentum part for \mathbb{R}_{base} with $n \in 2\mathbb{Z} + 1$ in (2.11). The states invariant under the twist are obtained in such a way that these signs are cancelled with each other.

In the following, we consider the ten-dimensional massless strings which belong to the untwisted sector (of the internal T_{fiber}^4 part) with $w, n \in 2\mathbb{Z}$ in (2.11), as simple examples to probe the interactions on the T-fold. With the left-moving fermions included, the relevant part of the partition function reads $(F_{(0,0)}^{T^4} \overline{f_{(0,0)}} + F_{(0,1)}^{T^4} \overline{f_{(0,1)}}) \mathcal{J}$. We also concentrate on the NS-NS sector. Massless strings involving the Ramond sectors are related by supersymmetry. The conjugacy class including the NS-NS massless states is then labeled as

$$\left[\text{o}(\overline{\text{oo}}) \right]_X \times \left[\text{v}(\overline{\text{vo}}) \right]_\psi. \tag{3.3}$$

The part inside $[\]_X$ is from $F_{(w,m)}^{T^4}$. For the fermion part $[\]_\psi$, we have denoted the conjugacy classes in the order of $[\psi_L^M(\psi_R^\mu, \psi_R^a)]$ ($M = 2, \dots, 9; \mu = 2, \dots, 5; a = 6, \dots, 9$). In the states of the massless strings, the excited non-zero modes are $(\psi_L)_{-1/2}^M$ and $(\psi_R)_{-1/2}^\mu$ only. Before taking the invariant combination of the momenta, they are thus expressed as

$$(\psi_L)_{-1/2}^M |0; K_L\rangle \otimes (\psi_R)_{-1/2}^\mu |0; K_R\rangle, \tag{3.4}$$

where $|0; K_{L/R}\rangle$ are the oscillator vacua with the ten-dimensional momenta,

$$K_L^M = (k_L^\mu, p_L^a), \quad K_R^M = (k_R^\mu, p_R^a), \tag{3.5}$$

whose components are moreover split into

$$k_L^\mu = (k^{\tilde{\mu}}, k_L^p), \quad k_R^\mu = (k^{\tilde{\mu}}, k_R^p), \tag{3.6}$$

with $\tilde{\mu} = 0, \dots, 3$ and $p = 4, 5$. For the conjugacy classes in (3.3), the momenta $p_{L/R}^a$ for $X_{L/R}^a$ take the value on the root lattice,

$$p_{L/R}^a = \sqrt{\frac{2}{\alpha'}} e_i^a m_{L/R}^i \quad (m_{L/R}^i \in \mathbb{Z}). \tag{3.7}$$

The momenta along X^p generally take the form,

$$k_L^p = \frac{n_p}{R_p} + \frac{w^p R_p}{\alpha'}, \quad k_R^p = \frac{n_p}{R_p} - \frac{w^p R_p}{\alpha'}, \tag{3.8}$$

where $n_5 \in \mathbb{Z}/2$ as in (2.11), $n_4, w^4, w^5 \in \mathbb{Z}$, and R_4 is the compactification radius for X^4 . In this notation, $n_5 \in \mathbb{Z}$, $w^5 \in 2\mathbb{Z}$ for the states in (3.4). Because of the on-shell condition, these states are indeed massless from the ten-dimensional point of view. Together with the level-matching condition, the momenta satisfy

$$K_L \cdot K_L := \eta_{MN} K_L^M K_L^N = 0, \quad K_R \cdot K_R := \eta_{MN} K_R^M K_R^N = 0. \quad (3.9)$$

These strings are regarded as those obtained from the four-dimensional massless strings by exciting the momenta along $S^1 \times \mathbb{R}_{\text{base}} \times T_{\text{fiber}}^4$, which make them massive from the four-dimensional point of view.

The corresponding vertex operators are constructed in a standard manner. In the $(-1, -1)$ picture, they are given by⁴

$$V_{\text{ut};p_R}^{(-1,-1)} = g_c e^{-\phi_L - \phi_R} \zeta_M \psi_L^M \bar{\zeta}_\mu \psi_R^\mu e^{iK_L \cdot X_L + iK_R \cdot X_R}, \quad (3.10)$$

where g_c is the coupling constant, $\zeta_M, \bar{\zeta}_\mu$ represent the polarizations satisfying $K_L^M \zeta_M = k_R^\mu \bar{\zeta}_\mu = 0$, and $k_R \cdot X_R := \eta_{\mu\nu} k_R^\mu X_R^\nu$. $\phi_{L,R}$ are the bosonized superconformal ghosts with the normalization, $\phi_L(z)\phi_L(0) \sim -\ln z$, $\phi_R(\bar{z})\phi_R(0) \sim -\ln \bar{z}$. We have explicitly denoted the dependence of $V_{\text{ut};p_R}^{(-1,-1)}$ on p_R^α . Acting with the modes of the supercurrents, one also obtains the vertex operators in the $(0, 0)$ picture,

$$\begin{aligned} V_{\text{ut};p_R}^{(0,0)} & \quad (3.11) \\ & = -\frac{2g_c}{\alpha'} \zeta_M \left(i\partial X_L^M + \frac{1}{2}\alpha' (K_L \cdot \psi_L) \psi_L^M \right) \bar{\zeta}_\mu \left(i\partial X_R^\mu + \frac{1}{2}\alpha' (K_R \cdot \psi_R) \psi_R^\mu \right) e^{iK_L \cdot X_L + iK_R \cdot X_R}. \end{aligned}$$

To make the states invariant under the twist σ , we further take the even combination of the states with p_R and $-p_R$. The corresponding vertex operator is denoted e.g. by

$$V_{\text{inv};p_R}^{(0,0)} := \frac{1}{\sqrt{2}} \left(V_{\text{ut};p_R}^{(0,0)} + V_{\text{ut};-p_R}^{(0,0)} \right). \quad (3.12)$$

3.3 Massless strings in the twisted sector

For the twisted sector, the conjugacy classes in $F_{(1,m)}^{T^4}$ for the left-mover are specified by the momentum p_L as in the untwisted sector. However, p_R in the right-mover vanishes. On dimensional grounds, one finds that \bar{o}/\bar{v} stands for the states with an even/odd number of excitations of $\tilde{\alpha}_{-(1/2+k)}^a$ ($k \in \mathbb{Z}_{>0}$), whereas \bar{s}, \bar{c} stand for those corresponding to their excitations above the twist fields. As in the untwisted sector, the invariant states are obtained in such a way that the signs due to the twist are cancelled with each other.

For the twisted sector (of the internal T_{fiber}^4 part), we consider the ten-dimensional massless strings which belong to the sector with $w \in 2\mathbb{Z} + 1$ and $n \in 2\mathbb{Z}$ in (2.11). The relevant part of the partition function reads $(F_{(1,0)}^{T^4} \overline{f_{(1,0)}} + F_{(1,1)}^{T^4} \overline{f_{(1,1)}}) \mathcal{J}$. We concentrate on the NS-NS sector with respect to the fermions ψ_L^M ($M = 2, \dots, 9$) and ψ_R^μ ($\mu = 2, \dots, 5$)

⁴We have omitted the cocycles for the toroidal compactification. They give extra phases in the amplitudes below, which are however irrelevant in our discussion.

without the twist.⁵ The conjugacy class including the NS-NS massless states is then labeled as

$$\left[\text{o}(\overline{\text{oc}}) \right]_X \times \left[\text{v}(\overline{\text{os}}) \right]_\psi. \quad (3.13)$$

The left-moving part is the same as in (3.3). The conjugacy class \bar{c} for X_R^a should include, as mentioned above, the states which correspond to the twist field $\Sigma_R(\bar{z}) = \prod_{a=6}^9 \Sigma_a(\bar{z})$ implementing the chiral reflection (2.1) and its dual $\bar{\Sigma}_R(\bar{z})$, and the excited ones above them. Here, Σ_a are the twist fields for X_R^a with dimension 1/16, and regarded as the twist fields of the type in the Ashkin-Teller model [20–27]. In appendix 8, we summarize the properties of those twist fields which are used below. For ψ_R^μ , the conjugacy class $\bar{\text{os}}$ represents the states corresponding to the twist fields \hat{S}_R^α with dimension 1/4, and the excited ones above them.

The spectrum in the partition functions $F_{(w,m)}^{T^4}$ in (3.2) can be represented by free fermions. In that case, the T-duality twist on X_R^a is represented similarly to (2.8) by the corresponding free bosons through bosonization. Such a representation would simplify the computations of scattering amplitudes. However, those free bosons are related non-locally to the original bosons X_R^a , and thus the physical interpretation of the results is not clear as they stand. We thus do not take this route in the following. The problem is essentially equivalent to the “bosonization” of the twist fields Σ_a . For a recent discussion in this respect, see [27].

In the $(-1, -1)$ picture, the corresponding vertex operators are then,

$$V_{\text{tw}}^{(-1,-1)} = g'_c e^{-\phi_L - \phi_R} \zeta_M \psi_L^M \bar{u}_\alpha \hat{S}_R^\alpha \Sigma_R e^{iK_L \cdot X_L + iK_R \cdot X_R}, \quad (3.14)$$

or those with $\bar{\Sigma}_R$ instead of Σ_R , which we denote by $\bar{V}_{\text{tw}}^{(-1,-1)}$. Here, g'_c is the coupling and \bar{u}_α is the polarization of the spinor. We denote the momenta $K_{L,R}$ again by the same form as in (3.5)–(3.8). From the physical state conditions, one finds that the corresponding states are massless from the ten-dimensional point of view, and

$$K_L \cdot K_L = K_R \cdot K_R = 0. \quad (3.15)$$

In the notation (3.8), the momenta $k_{L,R}^5$ of these states have $n_5 \in \mathbb{Z}$, $w^5 \in 2\mathbb{Z} + 1$, whereas the momenta p_L^a are on the root lattice and p_R^a are vanishing due to the twist,

$$p_L^a = \sqrt{\frac{2}{\alpha'}} e_i^a m_L^i \quad (m_L^i \in \mathbb{Z}), \quad p_R^a = 0. \quad (3.16)$$

The strings which we are considering are regarded as those obtained from the ground states, or the six-dimensional massless states outside T_{fiber}^4 , in the twisted sector by exciting the internal momenta. They are massive from the four-dimensional point of view.

As in the case of symmetric orbifolds, each twisted sector and hence each twist field may be associated to a fixed point under the chiral reflection (2.1). Thus, the vertex operators

⁵Though the NS and Ramond sectors are mixed due to the twist, the periodicity of the matter supercurrent $T_{F;R}^m$ in the right-mover does not change since the boundary conditions of X_R^a and ψ_R^a are changed simultaneously. The NS/Ramond sector of the matter part with respect to ψ_R^μ thus couples to the NS/Ramond sector of the superconformal ghosts, and thus the BRST symmetry is maintained.

generally include the fields which implement the shifts among the fixed points [28]. In the following, we work in a twisted sector with the same fixed point for simplicity, and assume that the twist field Σ_R is associated to it.⁶

4 Amplitudes with vanishing right-moving internal momenta

Now, we are ready to compute the amplitudes of the strings in the twisted and untwisted sectors whose vertex operators are constructed in the previous section. We focus on those of the NS-NS states as mentioned above. The amplitudes involving the Ramond states are related by supersymmetry. In particular, let us first consider the case where the right-moving internal momenta p_R 's along T_{fiber}^4 vanish also in the untwisted sector, while p_L 's are kept generic both in the twisted and untwisted sectors. This serves as a preparation for the case with non-vanishing p_R^a discussed in the next section, as well as a check of our computations there.

4.1 Three-point amplitudes involving the twisted sector

The untwisted NS-NS states in section 3.2 are invariant under the twist σ for the T-fold after taking the invariant combination of the momenta. The correlation functions and amplitudes only among them at the tree level are the same as those in the original model without the twist.

Once the twisted sector is involved, a non-vanishing three-point amplitude needs to include two twisted states, as they change the Hilbert space of the untwisted sector to that of the twisted sector, and vice versa. To saturate the ghost charge, the amplitude takes the form,

$$A_3^{(0)} = \left\langle c\bar{c}V_{\text{ut};p_R=0}^{(0,0)}(z_1) c\bar{c}\bar{V}_{\text{tw}}^{(-1,-1)}(z_2) c\bar{c}V_{\text{tw}}^{(-1,-1)}(z_3) \right\rangle, \quad (4.1)$$

with $c(z)$, $\bar{c}(\bar{z})$ being the ghosts. We note that $V_{\text{ut};p_R=0} = \frac{1}{\sqrt{2}}V_{\text{inv};p_R=0}$ for $p_R = 0$. Using the physical state conditions, one finds

$$\begin{aligned} A_3^{(0)} &= -(iC_{S^2})g_c g_c^2 a_3^L a_3^R (2\pi)^{10} \delta^{(10)}(K_1 + K_2 + K_3), \\ a_3^L &= -\sqrt{\frac{\alpha'}{2}} \zeta_{1M} \zeta_{2N} \zeta_{3K} t^{MNK}, \quad t^{MNK} := \eta^{MN} K_{L2}^K + \eta^{NK} K_{L3}^M + \eta^{KM} K_{L1}^N, \\ a_3^R &= -\sqrt{\frac{\alpha'}{2}} \bar{u}_{23} \bar{\zeta}_{1\mu} k_{R3}^\mu = \frac{1}{2} \sqrt{\frac{\alpha'}{2}} \bar{u}_{23} \bar{\zeta}_{1\mu} (k_{R2}^\mu - k_{R3}^\mu), \end{aligned} \quad (4.2)$$

where $\bar{u}_{ij} := \bar{u}_{i\alpha} \mathcal{C}^{\alpha\beta} \bar{u}_{j\beta} = \bar{u}_{i\alpha} \bar{u}_j^\alpha$ with $\mathcal{C}^{\alpha\beta}$ being (the chiral block of) the $\text{SO}(4)$ charge conjugation matrix, and a constant iC_{S^2} comes from the determinant of the Laplacian. $K_{L/Rj}$ is the left/right-moving momentum for the j -th vertex. Since $p_{Rj}^a = 0$ in the present

⁶The conjugacy class c of $\text{SO}(4)$ has two states with dimension $1/4$. A possible identification would be that each corresponds to Σ_R or $\bar{\Sigma}_R$. Another possibility would be that Σ_R is self-dual as in the Ashkin-Teller model, and one corresponds to Σ_R and the other to another twist field for another fixed point. The following discussion does not depend on details of the identification. See appendix 8. For the \mathbb{Z}_2 -symmetric orbifolds with Lie algebra lattices, the fixed points have been discussed in detail in [32].

case, $K_{Rj}^M = (k_{Rj}^\mu, 0)$. ζ_{jM} and $\bar{\zeta}_{j\mu}$ are the vector polarizations for the j -th vertex and, similarly, $\bar{u}_{j\alpha}$ are the spinor polarizations. Regarding the factors representing the momentum conservation, we normalize the states for the internal part without the volume factor as for the partition function (2.10), and thus $(2\pi)\delta(K^p)$ for S^1 or \mathbb{R}_{base} and $(2\pi)^4 \prod_{a=6}^9 \delta(K^a)$ for T_{fiber}^4 stand for $\delta_{n_p,0} \delta_{w^p,0}$ ($p = 4, 5$) and $\prod_j \delta_{m_L^j,0}$, respectively.

4.2 Four-point amplitudes

Let us move on to the computation of the four-point amplitudes. The number of the twisted states therein should be even, as in the three-point amplitudes. We thus consider

$$A_4^{(0)} = \left\langle c\bar{c}V_{\text{ut};0}^{(0,0)}(z_1) \int d^2z_2 V_{\text{ut};0}^{(0,0)}(z_2) c\bar{c}\bar{V}_{\text{tw}}^{(-1,-1)}(z_3) c\bar{c}V_{\text{tw}}^{(-1,-1)}(z_4) \right\rangle, \quad (4.3)$$

where we have set $p_R^a = 0$ for the untwisted states, and hence $p_{Rj}^a = 0$ ($j = 1, \dots, 4$). The computation of $A_4^{(0)}$ is straightforward though needs some algebra. For definiteness and later use, we list the result in some detail. First, by setting $z_1 = 1$, $z_2 = z$, $z_3 \rightarrow \infty$ and $z_4 = 0$, one finds

$$A_4^{(0)} = (iC_{S^2})(g_c g'_c)^2 \times (2\pi)^{10} \delta^{(10)}\left(\sum_{a=1}^4 K_a\right) \times I_4^{(0)}, \quad (4.4)$$

where

$$\begin{aligned} I_4^{(0)} &= \int d^2z D_{4;L}(z) D_{4;R}^{(0)}(\bar{z}), \\ D_{4;L} &= e^{-\pi i \left(1 + \frac{\alpha'}{2} K_{L3} \cdot K_{L4}\right)} z^{\frac{\alpha'}{2} K_{L2} \cdot K_{L4}} (1-z)^{\frac{\alpha'}{2} K_{L1} \cdot K_{L2}} \cdot \frac{\alpha'}{2} \left(\frac{A}{(1-z)^2} + \frac{B}{1-z} + \frac{C}{z} \right), \\ D_{4;R}^{(0)} &= e^{+\pi i \left(1 + \frac{\alpha'}{2} k_{R3} \cdot k_{R4}\right)} \bar{z}^{\frac{\alpha'}{2} k_{R2} \cdot k_{R4}} (1-\bar{z})^{\frac{\alpha'}{2} k_{R1} \cdot k_{R2}} \cdot \frac{\alpha'}{2} \left(\frac{\bar{A}^{(0)}}{(1-\bar{z})^2} + \frac{\bar{B}}{1-\bar{z}} + \frac{\bar{C}}{\bar{z}} \right), \end{aligned} \quad (4.5)$$

with

$$\begin{aligned} A &= \zeta_{12} \zeta_{34} \left(\frac{2}{\alpha'} - K_{L1} \cdot K_{L2} \right), \\ B &= (K_{L1} \cdot K_{L2}) (\zeta_{14} \zeta_{23} - \zeta_{13} \zeta_{24}) + \zeta_{12} (\kappa_{32} \kappa_{41} - \kappa_{31} \kappa_{42}) + \zeta_{34} (\kappa_{12} \kappa_{24} - \kappa_{14} \kappa_{21}) \\ &\quad - \zeta_{13} \kappa_{21} \kappa_{43} + \zeta_{14} \kappa_{21} \kappa_{34} + \zeta_{23} \kappa_{12} \kappa_{43} - \zeta_{24} \kappa_{12} \kappa_{34}, \\ C &= -(K_{L1} \cdot K_{L2}) \zeta_{13} \zeta_{24} + \zeta_{13} (\kappa_{21} \kappa_{42} - \kappa_{24} \kappa_{41}) + \zeta_{24} (\kappa_{12} \kappa_{31} - \kappa_{13} \kappa_{32}) \\ &\quad - \zeta_{12} \kappa_{31} \kappa_{42} + \zeta_{14} \kappa_{31} \kappa_{24} + \zeta_{23} \kappa_{13} \kappa_{42} - \zeta_{34} \kappa_{13} \kappa_{24}, \\ \bar{A}^{(0)} &= \bar{\zeta}_{12} \bar{u}_{34} \left(\frac{2}{\alpha'} - k_{R1} \cdot k_{R2} \right), \quad \bar{B} = \bar{u}_{34} (\bar{\kappa}_{12} \bar{\kappa}_{24} - \bar{\kappa}_{21} \bar{\kappa}_{14}), \quad \bar{C} = -\bar{u}_{34} \bar{\kappa}_{13} \bar{\kappa}_{24}. \end{aligned} \quad (4.6)$$

The dot (\cdot) stands for the contraction by η_{MN} in the left-mover, and that by $\eta_{\mu\nu}$ in the right-mover. To lighten the notation, we have introduced

$$\zeta_{ij} := \zeta_i \cdot \zeta_j, \quad \bar{\zeta}_{ij} := \bar{\zeta}_i \cdot \bar{\zeta}_j, \quad \kappa_{ij} := \zeta_i \cdot K_{Lj}, \quad \bar{\kappa}_{ij} := \bar{\zeta}_i \cdot k_{Rj}. \quad (4.7)$$

The above integral is evaluated by the formula (9.1) in appendix 9, which results in

$$I_4^{(0)} = (-1)^{n_s} I(\alpha, \beta; n_t, n_s) \cdot a_{4;L} a_{4;R}^{(0)}, \quad (4.8)$$

where

$$I(\alpha, \beta; n_t, n_s) = 2\pi (-1)^{1+n_u} \frac{\frac{\alpha'}{4} s_L \cdot \frac{\alpha'}{4} t_L \cdot \frac{\alpha'}{4} s_R \cdot \frac{\alpha'}{4} t_R}{\left(1 + \frac{\alpha'}{4} u_L\right) \left(1 + \frac{\alpha'}{4} u_R\right)} \frac{\Gamma\left(-\frac{\alpha'}{4} s_R\right) \Gamma\left(-\frac{\alpha'}{4} t_R\right) \Gamma\left(-\frac{\alpha'}{4} u_R\right)}{\Gamma\left(1 + \frac{\alpha'}{4} s_L\right) \Gamma\left(1 + \frac{\alpha'}{4} t_L\right) \Gamma\left(1 + \frac{\alpha'}{4} u_L\right)},$$

$$a_{4;L} = 2 \cdot \left(1 + \frac{\alpha'}{4} u_L\right) \left[\frac{u_L}{s_L \left(\frac{4}{\alpha'} + s_L\right)} A - \frac{1}{s_L} B - \frac{1}{t_L} C \right], \quad (4.9)$$

$$a_{4;R}^{(0)} = 2 \bar{u}_{34} \cdot \left(1 + \frac{\alpha'}{4} u_R\right) \left[\frac{u_R}{s_R \left(\frac{4}{\alpha'} + s_R\right)} \bar{A}^{(0)} - \frac{1}{s_R} \bar{B} - \frac{1}{t_R} \bar{C} \right],$$

with

$$\alpha = \alpha' K_{L2} \cdot K_{L4} = -\frac{\alpha'}{2} t_L, \quad \beta = \alpha' K_{L1} \cdot K_{L2} = -\frac{\alpha'}{2} s_L. \quad (4.10)$$

We have also defined

$$\begin{aligned} s_L &:= -(K_{L1} + K_{L2})^2, & t_L &:= -(K_{L1} + K_{L3})^2, & u_L &:= -(K_{L1} + K_{L4})^2, \\ s_R &:= -(k_{R1} + k_{R2})^2, & t_R &:= -(k_{R1} + k_{R3})^2, & u_R &:= -(k_{R1} + k_{R4})^2, \end{aligned} \quad (4.11)$$

and

$$n_s := \frac{\alpha'}{4} (s_L - s_R), \quad n_t := \frac{\alpha'}{4} (t_L - t_R), \quad n_u := \frac{\alpha'}{4} (u_L - u_R). \quad (4.12)$$

From (3.7), (3.8) and (3.16), these n_s, n_t, n_u are integers. The Mandelstam variables satisfy

$$s_L + t_L + u_L = 0, \quad s_R + t_R + u_R = 0, \quad (4.13)$$

which also implies $n_s + n_t + n_u = 0$. Substituting these into (4.4) gives $A_4^{(0)}$.

By rescaling, the polarization part is rewritten as

$$\begin{aligned} \tilde{a}_{4;L} &:= \frac{\frac{\alpha'}{4} s_L \cdot \frac{\alpha'}{4} t_L}{\left(1 + \frac{\alpha'}{4} u_L\right)} a_{4;L} \\ &= \frac{\alpha'^2}{8} \left[\frac{1}{2} u_L s_L \zeta_{13} \zeta_{24} - t_L (\zeta_{12} \kappa_{32} \kappa_{41} + \zeta_{14} \kappa_{21} \kappa_{34} + \zeta_{23} \kappa_{12} \kappa_{43} + \zeta_{34} \kappa_{14} \kappa_{23}) \right. \\ &\quad \left. + (\text{terms with } 2 \leftrightarrow 3) + (\text{terms with } 3 \leftrightarrow 4) \right], \end{aligned} \quad (4.14)$$

$$\tilde{a}_{4;R}^{(0)} := \frac{\frac{\alpha'}{4} s_R \cdot \frac{\alpha'}{4} t_R}{\left(1 + \frac{\alpha'}{4} u_R\right)} a_{4;R}^{(0)} = \frac{\alpha'^2}{8} \bar{u}_{34} \left(\frac{1}{2} t_R u_R \bar{\zeta}_{12} - t_R \bar{\kappa}_{14} \bar{\kappa}_{23} - u_R \bar{\kappa}_{13} \bar{\kappa}_{24} \right).$$

The left-moving part $\tilde{a}_{4;L}$ is symmetric with respect to s_L, t_L, u_L , and agrees with the standard expression for the massless scattering [33, 34]. The amplitude is also expressed in a Kawai-Lewellen-Tye (KLT)-like form [35] through,

$$I_4^{(0)} = \tilde{a}_{4;L} \tilde{a}_{4;R}^{(0)} \cdot 2(-1)^{n_s} \sin\left(\frac{\pi\alpha'}{4}s_L\right) \frac{\Gamma\left(-\frac{\alpha'}{4}s_L\right)\Gamma\left(-\frac{\alpha'}{4}u_L\right)}{\Gamma\left(1+\frac{\alpha'}{4}t_L\right)} \frac{\Gamma\left(-\frac{\alpha'}{4}s_R\right)\Gamma\left(-\frac{\alpha'}{4}t_R\right)}{\Gamma\left(1+\frac{\alpha'}{4}u_R\right)}. \quad (4.15)$$

For comparison with the result in the next section, let us note some properties of the amplitude. First, $A_4^{(0)}$ has the poles in the s -channel at

$$\frac{\alpha'}{4}s_L - n_s = \frac{\alpha'}{4}s_R = k \quad (k \in \mathbb{Z}_{\geq 0}) \quad (4.16)$$

for $n_s \geq 0$, whereas at

$$\frac{\alpha'}{4}s_R - |n_s| = \frac{\alpha'}{4}s_L = k \quad (k \in \mathbb{Z}_{\geq 0}) \quad (4.17)$$

for $n_s < 0$. The poles in the t - and u -channels are similar.

In the hard-scattering limit,

$$s_{L/R} \rightarrow \infty, \quad \frac{t_{L/R}}{s_{L/R}} : \text{fixed}, \quad (4.18)$$

with n_s, n_t, n_u also fixed for simplicity, one finds the asymptotic form,

$$\log A_4^{(0)} \sim \log A_{4;L}^{(0)} + \log A_{4;R}^{(0)}, \quad (4.19)$$

where $\log A_{4;L/R}^{(0)}$ comes from the left/right-mover and is given by

$$\log A_{4;L/R}^{(0)} \sim -\frac{\alpha'}{4} \left(s_{L/R} \log s_{L/R} + t_{L/R} \log t_{L/R} + u_{L/R} \log u_{L/R} \right). \quad (4.20)$$

This behavior is obtained by evaluating the saddle point value of the integrand of $I_4^{(0)}$ [36]. Although the Lorentz symmetry is absent for the internal part $K_{L/R}^M$ ($M = 4, \dots, 9$), let us further suppose for simplicity that e.g. the left-moving spatial momenta $\vec{K}_L = (K_L^M)$ ($M = 1, \dots, 9$) satisfy

$$0 = \vec{K}_{L1} + \vec{K}_{L2} = -\left(\vec{K}_{L3} + \vec{K}_{L4}\right), \quad (4.21)$$

for the scattering process $1+2 \rightarrow 3+4$, as in the usual center-of-mass frame. In this case,⁷

$$s_L = 4K^2, \quad t_L = -2K^2(1 + \cos\theta), \quad u_L = -2K^2(1 - \cos\theta), \quad (4.22)$$

with $K := |\vec{K}_{Lj}|$ ($j = 1, \dots, 4$). The left-moving part of (4.20) then becomes

$$\log A_{4;L}^{(0)} \sim -\alpha' K^2 f(\theta), \quad (4.23)$$

⁷We take all the spacial momenta to be positive when they are incoming.

where θ is the angle between \vec{K}_{L1} and \vec{K}_{L3} defined via $\vec{K}_{L1} \cdot \vec{K}_{L3} = K^2 \cos \theta$, and

$$f(\theta) = -\cos^2 \frac{\theta}{2} \cdot \log \left(\cos^2 \frac{\theta}{2} \right) - \sin^2 \frac{\theta}{2} \cdot \log \left(\sin^2 \frac{\theta}{2} \right), \quad (4.24)$$

as in the standard case. In the Regge limit,

$$s_{L/R} \rightarrow \infty, \quad t_{L/R}, n_s, n_t, n_u : \text{fixed}, \quad (4.25)$$

one also finds

$$\log A_{4;L/R}^{(0)} \sim \frac{\alpha'}{4} t_{L/R} \log s_{L/R}. \quad (4.26)$$

In the limit $|s_{L/R}|, |u_{L/R}| \gg |t_{L/R}|$, (4.20) reduces to (4.26).

5 Amplitudes with non-vanishing right-moving internal momenta

Based on the discussion in the previous section, we now consider the general amplitudes where the right-moving internal momenta p_{Rj} along T_{fiber}^4 are non-vanishing in the untwisted sector, while p_{Lj} are kept generic as before. The behavior of the amplitudes is indeed changed due to the T-duality twist.

5.1 Three-point amplitudes

When $p_R \neq 0$ in the untwisted sector, the three-point amplitude involving the twisted sector becomes

$$A_3 = \left\langle c\bar{c}V_{\text{inv};p_{R1} \neq 0}^{(0,0)}(z_1) c\bar{c}\bar{V}_{\text{tw}}^{(-1,-1)}(z_2) c\bar{c}V_{\text{tw}}^{(-1,-1)}(z_3) \right\rangle. \quad (5.1)$$

This is evaluated by using the correlator (8.2) in appendix 8. As discussed shortly, the coupling g_c also comes to dependent on p_R , which we denote as $g_c(p_R)$. Up to the coupling part, the result of A_3 is then given by a combination of $A_3^{(0)}$ in (4.2) weighted by the phases $e^{\pm i\bar{x}_0 \cdot p_{R1}}$,

$$A_3 = \frac{1}{\sqrt{2}} (e^{i\bar{x}_0 \cdot p_{R1}} + e^{-i\bar{x}_0 \cdot p_{R1}}) \times \frac{g_c(p_R)}{g_c(0)} A_3^{(0)}, \quad (5.2)$$

where $\bar{x}_0 \cdot p_{R1} := \delta_{ab} \bar{x}_0^a \cdot p_{R1}^b$, and \bar{x}_0^a is the zero-mode of the twisted sector which we are working in. As explained in the appendix, the momentum conservation is not imposed on p_R .

Supposed that the period of X_R^a is half that of $X^a = X_L^a + X_R^a$, which is given below (2.5), the periodicity of X_R^a is represented as $X_R^a \sim X_R^a + \sqrt{\alpha'/2} \cdot \pi e_k^a$ for each $k = 6, \dots, 9$. The fixed points under the twist $X_R^a \rightarrow -X_R^a$ are then at $\bar{x}_0^a = \sqrt{\alpha'/2} \cdot (\pi/2) \sum_{k=6}^9 \epsilon_k e_k^a$ where $\epsilon_k = 0, 1$. From (3.7), the phase $e^{2i\bar{x}_0 \cdot p_{R1}}$ becomes of the form $(-1)^m$ with $m \in \mathbb{Z}$ in this case.

5.2 Four-point amplitudes

We now consider the four-point amplitude,

$$A_4 = \left\langle c\bar{c}V_{\text{inv};p_{R1}}^{(0,0)}(z_1) \int d^2z_2 V_{\text{inv};p_{R2}}^{(0,0)}(z_2) c\bar{c}V_{\text{tw};0}^{(-1,-1)}(z_3) c\bar{c}V_{\text{tw};0}^{(-1,-1)}(z_4) \right\rangle, \quad (5.3)$$

with $p_{R1}, p_{R2} \neq 0$. The computation of the left-moving part is the same as in the previous section. For the right-moving part, by using the correlator in (8.3) we first compute the amplitudes with $V_{\text{ut};p_{Rj}}^{(0,0)}$ instead of $V_{\text{inv};p_{Rj}}^{(0,0)}$ ($j = 1, 2$), which we denote by $A_4^{p_{R1}, p_{R2}}$, and then sum up them. The computation of $A_4^{p_{R1}, p_{R2}}$ is similar to that in the previous case with $p_R = 0$, but with some differences: firstly, $\langle \prod e^{ik_{Rj} \cdot X_R} \rangle \langle \bar{\Sigma}_R \Sigma_R \rangle$ is replaced with

$$\begin{aligned} & \left\langle \prod e^{ik_{Rj} \cdot X_R} \right\rangle \left\langle e^{ip_{R1} \cdot X_R} e^{ip_{R2} \cdot X_R} \bar{\Sigma}_R \Sigma_R \right\rangle \\ &= e^{i\bar{x}_0 \cdot (p_{R1} + p_{R2})} \times \bar{z}_{34}^{-\frac{1}{2}} (\bar{z}_{12} \bar{z}_{34})^{-\frac{\alpha'}{4} s'_R} (\bar{z}_{13} \bar{z}_{24})^{-\frac{\alpha'}{4} t_R} (\bar{z}_{14} \bar{z}_{23})^{-\frac{\alpha'}{4} u_R} \left(\frac{1 - \sqrt{\bar{\xi}}}{1 + \sqrt{\bar{\xi}}} \right)^{\frac{\alpha'}{2} p_{R1} \cdot p_{R2}}, \end{aligned} \quad (5.4)$$

where $p_{R1} \cdot X_R := \delta_{ab} p_{R1}^a X_R^b$, $p_{Ri} \cdot p_{Rj} := \delta_{ab} p_{Ri}^a p_{Rj}^b$ and $\bar{\xi} := \bar{z}_{13} \bar{z}_{24} / \bar{z}_{23} \bar{z}_{14}$. The last factor is understood as due to the twisted propagator in (8.5). We have also defined

$$s'_R := s_R + k_{R1}^2 + k_{R2}^2 = -2k_{R1} \cdot k_{R2} = -2k_{R3} \cdot k_{R4} - p_{R1}^2 - p_{R2}^2. \quad (5.5)$$

s_R, t_R and u_R are defined in (4.11). We note that e.g. $t_R = -2k_{R1} \cdot k_{R3} + p_{R1}^2$ due to $p_{R1} \neq 0$. The terms with $i\bar{\partial}X_R$ in the computation are changed similarly.

Secondly, the terms $p_{Rj} \cdot \psi_R$ from $K_{Rj} \cdot \psi_R$ ($j = 1, 2$) are not vanishing in the vertex $V_{\text{ut};p_R}^{(0,0)}$ in (3.11). Consequently, one has an extra term proportional to

$$\left\langle \psi_R^a(\bar{z}_1) \psi_R^b(\bar{z}_2) \hat{S}_R^\alpha(\bar{z}_3) \hat{S}_R^\beta(\bar{z}_4) \right\rangle = h_+(\bar{z}_j) \delta^{ab} \mathcal{C}^{\alpha\beta} - h_-(\bar{z}_j) \left(\mathcal{C} \gamma^{ab} \right)^{\alpha\beta}, \quad (5.6)$$

where the index structure on the right side is fixed by the symmetry. We have defined $\gamma^{ab} := \frac{1}{2}(\gamma^a \bar{\gamma}^b - \gamma^b \bar{\gamma}^a)$ with $\gamma^a, \bar{\gamma}^a$ being the chiral blocks of the SO(4) gamma matrices. Our conventions of those matrices are summarized in appendix 10. By considering specific cases of the indices, one finds the coordinate dependent factors $h_\pm(\bar{z}_j)$ to be [37]

$$h_\pm(\bar{z}_j) = \frac{1}{2\bar{z}_{12}\bar{z}_{34}^{\frac{1}{2}}} \left(\bar{\xi}^{\frac{1}{2}} \pm \bar{\xi}^{-\frac{1}{2}} \right). \quad (5.7)$$

This results in a change of the polarization factor,

$$\bar{A}^{(0)} \rightarrow \bar{A}(\bar{\xi}) := \bar{A}^{(0)} - q_- \bar{\xi}^{\frac{1}{2}} - q_+ \bar{\xi}^{-\frac{1}{2}}, \quad (5.8)$$

with

$$q_\pm := \frac{1}{2} \bar{\zeta}_{12} \left(\bar{u}_{34} (p_{R1} \cdot p_{R2}) \pm p_{R1}^a p_{R2}^b (\mathcal{C} \gamma_{ab})^{\alpha\beta} \bar{u}_{3\alpha} \bar{u}_{4\beta} \right). \quad (5.9)$$

After setting $\bar{z}_1 = 1$, $\bar{z}_2 = \bar{z}$, $\bar{z}_3 \rightarrow \infty$ and $\bar{z}_4 = 0$, we find that $I_4^{(0)}$ in (4.5) changes as

$$I_4^{(0)} \rightarrow I_4 = \int d^2z D_{4;L}(z) D_{4;R}(\bar{z}), \quad (5.10)$$

for $A_4^{p_{R1}, p_{R2}}$, where $D_{4;L}(z)$ is given in (4.5) and

$$D_{4;R} = e^{\pi i \left(1 - \frac{\alpha'}{4} s'_R\right)} \bar{z}^{-\frac{\alpha'}{4} t_R} (1 - \bar{z})^{-\frac{\alpha'}{4} s'_R} \left(\frac{1 - \sqrt{\bar{z}}}{1 + \sqrt{\bar{z}}}\right)^{\frac{\alpha'}{2} p_{R1} \cdot p_{R2}} \frac{\alpha'}{2} \left(\frac{\bar{A}(\bar{z})}{(1 - \bar{z})^2} + \frac{\bar{B}}{1 - \bar{z}} + \frac{\bar{C}}{\bar{z}}\right). \quad (5.11)$$

In the present case, the Mandelstam variables satisfy

$$s_L + t_L + u_L = 0, \quad s'_R + t_R + u_R = 0. \quad (5.12)$$

n_s, n_t, n_u defined in (4.12) remain to be integers. We also define

$$n'_s := \frac{\alpha'}{4} (s_L - s'_R) = n_s + \frac{\alpha'}{4} (p_{R1}^2 + p_{R2}^2), \quad (5.13)$$

which is also an integer satisfying $n'_s + n_t + n_u = 0$.

The integral I_4 is evaluated by using the results in appendix 9. We thus obtain

$$A_4^{p_{R1}, p_{R2}} = (iC_{S^2}) (g'_c)^2 g_c(p_{R1}) g_c(p_{R2}) \times (2\pi)^{10} \delta^{(10)} \left(\sum_{a=1}^4 K_a\right) \times e^{i\bar{x}_0 \cdot (p_{R1} + p_{R2})} I_4, \quad (5.14)$$

$$I_4 = 2\pi (-1)^{1+n'_s} \tilde{a}_{4;L} \times \frac{\Gamma\left(-\frac{\alpha'}{4} u_L\right)}{\Gamma\left(1 + \frac{\alpha'}{4} s_L\right) \Gamma\left(1 + \frac{\alpha'}{4} t_L\right)} \times b_{4;R},$$

$$b_{4;R} = \frac{\alpha'}{2} \left[J_R(\bar{\alpha}, \bar{\beta} - 2, \bar{\gamma}) \cdot \bar{A}^{(0)} - J_R\left(\bar{\alpha} + \frac{1}{2}, \bar{\beta} - 2, \bar{\gamma}\right) \cdot q_- - J_R\left(\bar{\alpha} - \frac{1}{2}, \bar{\beta} - 2, \bar{\gamma}\right) \cdot q_+ \right. \\ \left. + J_R(\bar{\alpha}, \bar{\beta} - 1, \bar{\gamma}) \cdot \bar{B} + J_R(\bar{\alpha} - 1, \bar{\beta}, \bar{\gamma}) \cdot \bar{C} \right],$$

where $J_R(\bar{\alpha}, \bar{\beta}, \bar{\gamma})$ is given in terms of the hypergeometric function as in (9.6), and

$$\bar{\alpha} = -\frac{\alpha'}{4} t_R, \quad \bar{\beta} = -\frac{\alpha'}{4} s'_R, \quad \bar{\gamma} = \frac{\alpha'}{2} p_{R1} \cdot p_{R2}. \quad (5.15)$$

We recall that $\tilde{a}_{4;L}$ is given in (4.14), and $\bar{A}^{(0)}, \bar{B}, \bar{C}$ are in (4.6). When $\bar{\gamma} = 0$, the integral I_4 reduces to $I_4^{(0)}$ in (4.8) due to (9.10), and so does $A_4^{p_{R1}, p_{R2}}$ to $A_4^{(0)}$. We note that $A_4^{-p_{R1}, -p_{R2}} = e^{-2i\bar{x}_0 \cdot (p_{R1} + p_{R2})} A_4^{p_{R1}, p_{R2}}$.

By combining $A_4^{\pm p_{R1}, \pm p_{R2}}$, we obtain the four-point amplitude for the invariant un-twisted states in (5.3),

$$A_4 = \frac{1}{2} \left(A_4^{p_{R1}, p_{R2}} + A_4^{p_{R1}, -p_{R2}} + A_4^{-p_{R1}, p_{R2}} + A_4^{-p_{R1}, -p_{R2}} \right). \quad (5.16)$$

This is our final result of the computation of A_4 .

5.3 Poles of the amplitudes

From the analytic structure of $J_R(\bar{\alpha}, \bar{\beta}, \bar{\gamma})$ explained in appendix 9, one finds that the possible poles of the amplitude A_4 are at

$$\frac{\alpha'}{4} u_L = m_u, \quad \frac{\alpha'}{4} t_R = \frac{1}{2} (m_t + l_t), \quad \frac{\alpha'}{4} (s'_R - 2p_{R1} \cdot p_{R2}) = m_s + l_s, \quad (5.17)$$

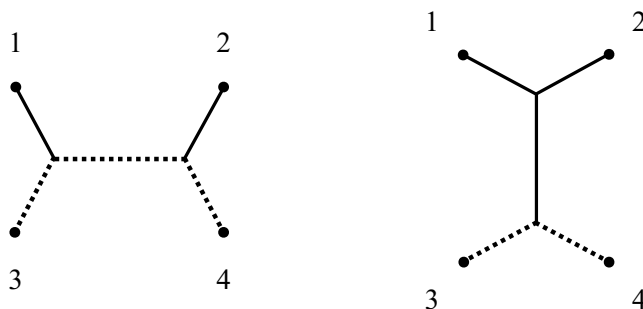


Figure 1. Emission of untwisted strings from twisted sector or t -channel picture of A_4 (left), and s -channel picture (right). The solid/dashed lines represent the propagation of the untwisted/twisted strings.

where $m_u, m_t, m_s \in \mathbb{Z}_{\geq 0}$, and $l_t = 0, 1, 2, 3$ and $l_s = -1, 0, 1$ are due to the shift of the arguments $\bar{\alpha}$ and $\bar{\beta}$ in J_R , respectively. Since $s'_R - 2p_{R1} \cdot p_{R2} = -2K_{R1} \cdot K_{R2} = -(K_{R1} + K_{R2})^2$, the poles are specified by the “proper” Mandelstam variable also in the s -channel. From the integral representation of I_4 as $\bar{z} \rightarrow 1$, or by using (9.17), one can check that the residue of the apparent unwanted tachyonic pole at $s'_R - 2p_{R1} \cdot p_{R2} = -4/\alpha'$ from $l_s = -1$ vanishes. The series at $\frac{\alpha'}{4}t_R - \frac{1}{2} = m \in \mathbb{Z}_{\geq 0}$ should be cancelled with the zeros coming e.g. from the hypergeometric functions in I_4 as in the case of $\bar{\gamma} = 0$; the amplitude is symmetric with respect to t_R and u_R , or the t -channel poles arise from the contributions around $\bar{z} \rightarrow 0$ which are irrelevant of the value of $\bar{\gamma}$. This agrees with the allowed intermediate states in this channel read off from the partition function (2.10). Thus, we are left with the possible poles at

$$\frac{\alpha'}{4}u_L = m'_u, \quad \frac{\alpha'}{4}t_R = m'_t, \quad \frac{\alpha'}{4}(s'_R - 2p_{R1} \cdot p_{R2}) = m'_s, \quad (5.18)$$

with $m'_u, m'_t, m'_s \in \mathbb{Z}_{\geq 0}$. Still, some may be cancelled with the zeros from other part of I_4 , as in the case of $\bar{\gamma} = 0$ described in section 4.2.

5.4 Suppression of the three-point coupling

In the presence of the two twist fields $\Sigma_R, \bar{\Sigma}_R$, the untwisted vertices are regarded as describing the emission of the untwisted states from the twisted sector, as in figure 1 (left). The factorization of A_4 shows that the coupling g_c in $V_{\text{ut};p_R}$ comes to depend on the momentum, as mentioned above, similarly to the case of symmetric orbifolds [28].

To see this, we note that the last factor in (5.4) from the twisted propagator is reduced to $[(1 - \sqrt{\bar{z}})/(1 + \sqrt{\bar{z}})]^{\frac{\alpha'}{2}p_{R1} \cdot p_{R2}}$ by setting $(\bar{z}_1, \bar{z}_2, \bar{z}_3, \bar{z}_4) = (1, \bar{z}, \infty, 0)$ as above. Though the denominator $1 + \sqrt{\bar{z}}$ does not change the short-distance singularity, it gives an extra factor in $[(1 - \bar{z})/4]^{\frac{\alpha'}{2}p_{R1} \cdot p_{R2}}$ for $\bar{z} \rightarrow 1$. We denote the coupling in the vertex for the emission from the untwisted sector by g_0 . Then, evaluating the contribution to A_4 from the integrand around $\bar{z} = 1$, and relating it to the product of the three-point amplitudes in the s -channel as in figure 1 (right), we find

$$A_4 \sim g_c(p_{R1}) g_c(p_{R2}) 2^{-\alpha' p_{R1} \cdot p_{R2}} \sim g_0 g_c(p_{R1} + p_{R2}). \quad (5.19)$$

Here, we have used $C_{S^2} \sim 1/g_0^2$ [38]. $g_c(p_R)$ is thus regarded as the three-point coupling among two twisted states and an untwisted state with internal momentum p_R . In the t -channel factorization, one indeed finds $A_4 \sim g_c(p_{R1}) g_c(p_{R2})$. The relation (5.19) is solved by

$$g_c(p_R) \sim 2^{-\frac{\alpha'}{2} p_R^2} g_0. \quad (5.20)$$

In the present case of an asymmetric orbifold, the coupling depends only on the right-moving momentum p_R . Moreover, it follows from (3.7) that

$$\frac{\alpha'}{2} p_R^2 = C_{ij} m_R^i m_R^j \in 2\mathbb{Z}, \quad (5.21)$$

where C_{ij} is the Cartan matrix of $SO(8)$, and hence the suppression factor of the coupling is quantized in integer powers of $1/4$. The momentum along a compactified direction with radius R_i has the winding contribution wR_i/α' as in (3.8), and $R_i/\sqrt{\alpha'}$ corresponds to the inverse coupling of the sigma model. Therefore, the factor $2^{-\alpha' p_R^2/2}$ in (5.20) includes stringy effects of the form $e^{-w^2 R_i^2/\alpha'}$ which are non-perturbative from the sigma-model point of view. The compactification radii in (2.4) are of order $\sqrt{\alpha'}$ and not explicit there. This suppression of the coupling implies that an untwisted string with large momentum p_R hardly interacts with twisted strings confined around the fixed point.

The suppression factor in (5.20) is also understood as a consequence of the normal ordering of the vertex operator e^{ipX} , and of the difference of the mode expansions for different boundary conditions by $n \in \mathbb{Z}$ or $n \in \mathbb{Z} + \frac{1}{2}$ [28]. The mechanism of the suppression is hence robust even for asymmetric orbifolds. The argument of the normal ordering is extended to the case of \mathbb{Z}_N orbifolds with $N > 2$. The suppression factor for $\mathbb{Z}_{N>2}$ symmetric orbifolds schematically takes the form $N^{-(\text{momenta})^2} \times (\text{factors depending on } N \text{ and momenta})$ [28, 39]. It is thus understood that the base 2 of $1/4 = 2^{-2}$ in our case comes from $\mathbb{Z}_{N=2}$ of the T-duality twist in the untwisted sector of the T_{fiber}^4 part, and the exponent 2 is from the length of the roots of $SO(8)$. The geometrical interpretation of the suppression in the symmetric case [28], however, may not apply as it stands, since we are considering a T-fold/asymmetric orbifold and in addition working in a twisted sector with the same fixed point.

5.5 High energy behaviors

From the expression (5.14), (5.16), one can read off high energy behaviors of the amplitude A_4 . The high energy limit corresponds to $\alpha' \rightarrow \infty$, which is opposite to the particle limit $\alpha' \rightarrow 0$. To see those behaviors, let us first summarize the kinematics. We denote the momenta as in (3.5)–(3.8), (3.16). Their conservation reads $0 = \sum_{j=1}^4 k_j^{\tilde{\mu}} = \sum_{j=1}^4 k_{L/Rj}^P = \sum_{j=1}^4 p_{Lj}^a$, whereas p_{Rj}^a with $p_{R3}^a = p_{R4}^a = 0$ do not have to be conserved. The momenta also have to satisfy the on-shell and level-matching conditions (3.9), (3.15). We mainly consider the scattering process $1 + 2 \rightarrow 3 + 4$. Other processes can be analyzed similarly, which we comment on below. By the Lorentz symmetry for $k^{\tilde{\mu}}$, one can then take the center-of-mass frame where

$$0 = \vec{k}_1 + \vec{k}_2 = -(\vec{k}_3 + \vec{k}_4), \quad (5.22)$$

with $\vec{k} = (k^1, k^2, k^3)$. A variety of high energy limits is allowed because of the asymmetry between the left- and the right-mover, the absence of the conservation of p_R and that of the Lorentz symmetry for $k_{L/R}^p$ and $p_{L/R}^a$ along $S^1 \times \mathbb{R}_{\text{base}} \times T_{\text{fiber}}^4$. In the following, we concentrate on the case characteristic to the strings on the T-fold where p_{R1}, p_{R2} are large and the T-duality twist has significant influence through the factor from the twisted propagator in (5.4).

Hard-scattering limit. As an example, we first consider a high-energy limit where the momenta of the untwisted strings along T_{fiber}^4 are large and those along other spatial directions are kept fixed:

$$|p_{L/R1}|, |p_{L/R2}| \gg |\vec{k}_j|, |k_{L/Rj}^p| \quad (j = 1, 2). \quad (5.23)$$

We also fix the internal momenta of the twisted strings $|k_{L/Rj}^p|$ ($j = 3, 4$) for simplicity. From the on-shell and level-matching conditions, it follows that $|p_{Lj}|$ ($j = 3, 4$) are fixed, and that

$$|p_{Rj}| \sim |p_{Lj}| \sim p \quad (j = 1, 2), \quad |k_j^0| \sim p \quad (j = 1, \dots, 4), \quad |\vec{k}_j| \sim p \quad (j = 3, 4), \quad (5.24)$$

with $p := |p_{R1}|$ being large. For this kinematic configuration, the Mandelstam variables are

$$\begin{aligned} s_L &\sim 4p^2, & t_L &\sim -2p^2, & u_L &\sim -2p^2, \\ s'_R &\sim 2p^2, & t_R &\sim -p^2, & u_R &\sim -p^2. \end{aligned} \quad (5.25)$$

Thus, sending $p \rightarrow \infty$ is a hard-scattering limit.

In this limit, the asymptotic form of the amplitude consists of the terms from the left- and the right-mover as in (4.19), and from the momentum-dependent couplings in this case,

$$\log A_4^{p_{R1}, p_{R2}} \sim \log A_{4;L} + \log A_{4;R}^{p_{R1}, p_{R2}} + \log [g_c(p_{R1})g_c(p_{R2})]. \quad (5.26)$$

The contribution from the left-mover comes from the factor $B^{-1}(-\alpha/2, -\beta/2)$ in (5.14) with (4.10), where $B(x, y)$ is the beta function, and remains the same as to $A_4^{(0)}$,

$$\log A_{4;L} \sim -\frac{\alpha'}{4}(s_L \log s_L + t_L \log t_L + u_L \log u_L) \sim -\alpha' p^2 \log 2. \quad (5.27)$$

Due to (5.20), the contribution from the couplings also becomes

$$\log [g_c(p_{R1})g_c(p_{R2})] \sim -\alpha' p^2 \log 2. \quad (5.28)$$

On the other hand, the contribution from the right-mover comes from the factor $J_R(\bar{\alpha}, \bar{\beta}, \bar{\gamma})$ in (5.14) with (5.15) and

$$\bar{\gamma} \sim \frac{\alpha'}{2} p^2 \cos \phi, \quad (5.29)$$

where ϕ is the angle between p_{R1}^a and p_{R2}^a . The behavior of this factor for $p \rightarrow \infty$ can be found by using the formulas of the hypergeometric function listed in appendix 9. Using (9.14) and (9.15), one finds

$$\begin{aligned} J_R(\bar{\alpha}, \bar{\beta}, \bar{\gamma}) &\sim 2B(2 - \bar{\beta}, 1 + \bar{\beta} + \gamma) F(2 - \bar{\beta}, \bar{\gamma} - \bar{\beta}; 3 + \bar{\gamma}; -1) \\ &= 2^{\bar{\beta}-1} B(2 - \bar{\beta}, 1 + \bar{\beta} + \gamma) F(2 - \bar{\beta}, 3 + \bar{\beta}; 3 + \bar{\gamma}; 1/2) \\ &\sim \left(\frac{\bar{\beta}}{2}\right)^{-\bar{\beta}} (\bar{\beta} + \bar{\gamma})^{\frac{\bar{\beta} + \bar{\gamma}}{2}} (\bar{\beta} - \bar{\gamma})^{\frac{\bar{\beta} - \bar{\gamma}}{2}}. \end{aligned} \tag{5.30}$$

Here, we have used

$$\bar{\alpha} \sim -\frac{1}{2}\bar{\beta}, \quad \bar{\gamma} \sim -\bar{\beta} \cos \phi, \tag{5.31}$$

and the fact that $F(a, b; c; z)$ is an entire function of a, b, c for $|z| < 1$ or $\text{Re } z < 1/2$ and hence $F(2 - \bar{\beta}, 3 + \bar{\beta}; 3 + \bar{\gamma}; 1/2) \sim F(-\bar{\beta}, 1 + \bar{\beta}; \bar{\gamma}; 1/2)$ for large $|\bar{\beta}|$. Thus, when (5.31) holds,

$$\begin{aligned} \log A_{4;R}^{p_{R1}, p_{R2}} &\sim -\frac{\alpha'}{4} (s'_R \log s'_R + t_R \log t_R + u_R \log u_R) - \frac{\alpha'}{4} s'_R [\log 2 - f(\phi)] \\ &\sim -\frac{\alpha'}{2} p^2 [2 \log 2 - f(\phi)], \end{aligned} \tag{5.32}$$

where $f(x)$ is the function defined in (4.24). This function is rewritten as $f(\phi) = \tilde{f}(\cos^2 \frac{\phi}{2})$ where $\tilde{f}(y) := -y \log y - (1 - y) \log(1 - y)$. Since $0 \leq \tilde{f}(y) \leq \log 2$ for $y \in [0, 1]$ with the maximum $\tilde{f}(1/2) = \log 2$ and the minima $\tilde{f}(0) = \tilde{f}(1) = 0$, one finds a bound,

$$4^{-\frac{\alpha'}{2} p^2} \lesssim A_{4;R}^{p_{R1}, p_{R2}} \lesssim 2^{-\frac{\alpha'}{2} p^2}. \tag{5.33}$$

When $\bar{\gamma} = 0$ or $\cos \phi = 0$, namely, when the factor from the twisted propagator in (5.4) disappears, $f(\phi)$ has the maximum $\log 2$ and the right-hand side of (5.32) reduces to the standard form in terms of s'_R, t_R and u_R as in (4.20). The angle dependence given by $f(\phi)$ is also the same as in (4.23). The sign of its coefficient $+\alpha' s'_R/4$ is, however, opposite to (4.23), so that the amplitude is more suppressed as $|\bar{\gamma}|$ becomes larger. The behaviors $A_{4;R}^{p_{R1}, p_{R2}} \sim 2^{-\alpha' p^2/2}, 4^{-\alpha' p^2/2}$ for $\cos \phi = 0$ ($\bar{\gamma} = 0$), $\cos \phi = \mp 1$ ($\bar{\gamma} = \pm \bar{\beta}$), respectively, are also confirmed from (9.9), (9.16) and (9.17), respectively.

The high-energy behavior in (5.30) is obtained also by the saddle point v_0 of the integrand of J_R in (9.6), which solves $(\bar{\alpha} + \bar{\beta})v^2 + \bar{\gamma}v - \bar{\alpha} = 0$. For the present kinematic configuration, the solutions are $v_0 \sim -y \pm i\sqrt{1 - y^2}$ with $y := \bar{\gamma}/\bar{\beta} \sim -\cos \phi$. One finds that the two saddle points give the same value of the integrand up to a phase depending on $\bar{\gamma}$, and that it agrees with (5.30). This means that the saddle-point argument in [36] may be developed also in our case of a T-fold. Our explicit computation shows in particular that both of the two saddle points are dominant, and one can take either of them up to the phase corresponding to the choice of the branch, but not their linear combinations.

We note that (5.32) in this limit is symmetric with respect to ϕ and $\pi - \phi$ or $\bar{\gamma}$ and $-\bar{\gamma}$ before summing up $\pm p_{Rj}$ as in (3.12) and (5.16). Therefore, in the asymptotic form of

the total amplitude A_4 denoted as in (5.26), the contribution from the right-mover $A_{4;R}$ corresponding to $A_{4;R}^{p_{R1}, p_{R2}}$ remains the same in this limit,

$$A_{4;R} \sim A_{4;R}^{p_{R1}, p_{R2}}. \tag{5.34}$$

With the help of the above saddle-point argument, this may be understood as follows: if we formulate our orbifold theory on the Riemann surface with the branch cut representing the twist, the summation of $\pm p_{Rj}$ is automatically taken care of (up to the zero-mode factors $e^{i\vec{x}_0 \cdot p_{Rj}}$), since moving to another sheet, $\sqrt{\bar{z}} \rightarrow -\sqrt{\bar{z}}$, flips the sign of $\bar{\gamma}$ in (5.4). In picking up a saddle point, global properties of the Riemann surface are not relevant, and thus it may reproduce the invariant result under $\bar{\gamma} \rightarrow -\bar{\gamma}$ or $\phi \rightarrow \pi - \phi$. In the usual hard scattering, this type of invariance corresponds to the symmetry between the t - and u -channels, which is represented e.g. by $f(\theta)$ in (4.20). This observation may partly explain why the same angle dependence $f(\phi)$ appears also in the present case.

It is also possible to consider the high-energy limit where $|\vec{k}_1| = |\vec{k}_2|$ becomes large in addition. The asymptotic form of the amplitude in this case would be obtained once the asymptotic form of the hypergeometric function in the general case is given, or it is supposed that picking up one saddle point gives the correct result as above.

For other processes, one can consider, for example, the $1 + 3 \rightarrow 2 + 4$ process where $|p_{Lj}| \sim |p_{Rj}| \sim p$ ($j = 1, 2$) are large and other momenta are fixed or vanishing. The contribution from the right-mover and that from the momentum-dependent couplings are dominant in this case. From the asymptotic form of J_R as above, it turns out that, as p increases, so does the former as opposed to (5.32), while the latter still decreases. Adding these together, one finds $\log A_4 \sim -\frac{\alpha'}{2} p^2 f(\phi)$, which takes a standard form for the hard scattering. This shows that the momentum dependence of the coupling ensures the soft behavior of the amplitudes in this case.

Regge-like limits. Next, we consider high-energy limits of the $1 + 2 \rightarrow 3 + 4$ process where all the Mandelstam variables do not become large. For simplicity, we suppose that \vec{K}_{Lj} with $p_{Lj} \neq 0$ also satisfy the same relations (4.21) and (4.22) as in the usual center-of-mass frame. Then,

$$s_L \rightarrow \infty, \quad t_L : \text{fixed} \quad (\cos \theta \rightarrow -1), \tag{5.35}$$

is a Regge(-like) limit. The contribution to the asymptotic form of A_4 from the left-mover takes the same form as $A_L^{(0)}$ in (4.26). The Mandelstam variables in the right-mover are

$$s'_R = 2K^2 + 2k^2 - 2k_{R1}^p k_{R2}^p, \quad t_R = -2K^2 + 2k^2 - 2k_{R1}^p k_{R3}^p + p_{R1}^2, \tag{5.36}$$

where we have set $K = |\vec{K}_{Lj}|$ and $k = |\vec{k}_{Lj}|$ ($j = 1, \dots, 4$). To be concrete, we take e.g. $p_L := |p_{Lj}|$ ($j = 1, \dots, 4$) to be large, and $(k_{Lj}^p)^2$ ($j = 1, \dots, 4$) and $(k_{Rj}^p)^2$ ($j = 1, 2$) to be fixed. In this case, $K^2 \sim k^2 + p_L^2$ and, from the level-matching condition, $p_L^2 \sim p_{R1}^2 \sim p_{R2}^2 \sim (k_{R3}^p)^2 \sim (k_{R4}^p)^2$, which results in⁸

$$s'_R \sim 2 \left(2k^2 + p_L^2 \right), \quad t_R \sim -p_L^2, \quad p_{R1} \cdot p_{R2} \sim p_L^2 \cos \phi. \tag{5.37}$$

⁸For generic radii R_p ($p = 4, 5$) in (3.8) where n_p and w^p are separately conserved, (4.21) and (5.35) imply $k_{L1}^p = k_{L4}^p = -k_{L2}^p = -k_{L3}^p$ and a similar relation for k_{Rj}^p . The latter relation for the right-mover, however, do not necessarily hold at special radii.

With these Mandelstam variables, the analysis of the contribution from the right-mover reduces to that for the hard-scattering limit discussed above.

One may also consider the high-energy limit where t_R instead of t_L is fixed. Though t_R is a fundamental variable of the amplitude, it is not a standard Mandelstam variable due to the existence of the internal momenta p_{Rj} . One finds that it is very restrictive to fix t_R for large p_{Rj} so as to be compatible with the momentum conservation, and the on-shell and level-matching conditions. We refrain from going into further details in such rather special cases.

6 Discussion

By taking a model of strings on T-folds as an example, we have discussed their interactions from the world-sheet point of view which are exact in α' . We have computed the three- and four-point amplitudes of a class of ten-dimensional massless strings both in the twisted and untwisted sectors. The four-point amplitudes are obtained in a closed form in terms of the hypergeometric function. From their factorization, it turns out that the three-point coupling among the twisted and untwisted strings is suppressed by the chiral momenta flowing along the T-folded internal torus, as in the case of general symmetric orbifolds. Furthermore, the coupling is quantized in integer powers of $1/4$ in our case of a T-fold, since the T-duality twist is \mathbb{Z}_2 in the untwisted sector of the torus part and the chiral momenta take the value on a Lie algebra lattice. The asymptotic forms of the four-point amplitudes in high-energy limits have also been found. These results include stringy effects which are non-perturbative from the sigma-model point of view, or those for $\alpha' \rightarrow \infty$ which is opposite to the particle limit $\alpha' \rightarrow 0$. They probe strings on a T-fold beyond the regime of supergravity and DFT.

For the strings other than those discussed in this paper, their vertex operators may be found by following the discussion in section 3, and their amplitudes may be obtained similarly. The momenta p_{Rj} along the internal torus generally take the value on the weight lattice, instead of the root lattice, of $SO(8)$, and hence the suppression factor of the coupling becomes integer powers of $1/2$, instead of $1/4$. By using the correlators involving more twist fields than those listed in appendix 8, one can also compute the amplitudes with more twisted strings. The simplest among these is the four-point amplitudes only of the strings excited above the ground states in the twisted sector by the internal momenta. In this case, however, the right-moving momenta p_{Rj} along the internal torus, a key ingredient of our analysis, are all vanishing. The amplitudes involving different twisted sectors may be computed by introducing the operators connecting them, as mentioned at the end of section 3.3.

As understood from the discussions so far, our analysis relies only on general properties of the T-duality twist and the symmetry enhancement of the internal torus, and hence may be extended qualitatively to more general T-folds. Furthermore, our analysis can be applied or extended to other asymmetric as well as symmetric orbifold models, including those mentioned in section 1 [13, 14, 16], which are based on the (chiral) reflection of the coordinate fields.

Compared with toroidally compactified models, where the left- and right-movers are not symmetric either, the appearance of the twisted propagator is characteristic to the present case of a T-fold or an asymmetric orbifold. This changes the expression of the amplitudes and results in the suppression of the coupling. The absence of the conservation of the momentum p_R along the twisted torus also affects the kinematics. Such properties are common to the case of symmetric orbifolds. Details are, however, different. For example, by extending the formula (9.7) as in (9.13), the four-point amplitudes may be obtained as a combination of the hypergeometric functions from the left and right movers. The exponent of the suppression factor in the symmetric case is given by the momenta in the untwisted sector as $p_L^2 + p_R^2$ [28] instead of p_R^2 . Since p_L and p_R differ by the root lattice as mentioned in section 2.1, these exponents can be largely different due to the windings w^j . As the left-mover is twisted in addition, the momentum p_L in the twisted sector vanishes, and its conservation in the untwisted sector does not need to hold. The left-moving part of the amplitudes may be given also by the variables which are defined similarly to s'_R, t_R, u_R in the right-mover. These change the kinematics significantly and, together with the difference of the spectrum, the amplitudes with large left-right asymmetry of the type discussed in section 5.5 may not appear. The analysis of the high-energy behavior of the amplitudes becomes different accordingly.

Our analysis in this paper demonstrates that strings on T-folds, which are very stringy and might appear to be unconventional, can be analyzed in a quantitative manner, once the world-sheet theory is properly given, even though its construction is rather involved. This may be regarded as an advantage of the world-sheet analysis. A future problem there would be to make “geometric” interpretations clearer regarding the fixed points, the associated twisted sectors, and the mechanism of the suppression of the coupling even for the non-geometric case of T-folds/asymmetric orbifolds.

Given the results which are valid for all α' , one may consider their applications to further studies of strings on T-folds and related ones. For example, since T-folds may be treated geometrically in DFT before it is reduced in the supergravity frame, it would be of interest to figure out the implications of our results in the structure of DFT including the α' -corrections [40] before the section condition is imposed. In addition, non-geometric fluxes are associated with weakly constrained DFT [41]. Thus, our results, or their extensions, would be used also to study its structure.⁹ Finally, the world-sheet for the four-point amplitudes discussed in this paper has the branch cut which is created by the twist fields and implements the T-duality twist. This branch cut may be regarded as a world-sheet conformal interface/defect [42–44] inducing T-duality. Conformal interfaces have properties which extend those of conformal boundaries or D-branes. Although there are related works [45–50], the role of world-sheet conformal interfaces in string theory, if any, is yet to be explored. It would be interesting if one could probe it by utilizing the results in this paper. We would like to discuss these issues further elsewhere.

⁹We would like to thank the referee for raising a question on this issue.

Acknowledgments

We would like to thank Y. Sakatani and S. Watamura for useful discussion. This work is supported in part by JSPS KAKENHI Grant Number JP17K05406.

7 Components of partition function

The components of the partition function in (2.10) are given by

$$Z_{(w,m)}^{\text{base}}(\tau, \bar{\tau}) := \frac{R_5}{\sqrt{\alpha' \tau_2} |\eta(\tau)|^2} e^{-\frac{\pi R_5^2}{\alpha' \tau_2} |w\tau + m|^2}, \quad (7.1)$$

$$\mathcal{J}(\tau) := \frac{1}{2} \left[\left(\frac{\theta_3}{\eta} \right)^4 - \left(\frac{\theta_4}{\eta} \right)^4 - \left(\frac{\theta_2}{\eta} \right)^4 \right] \equiv 0, \quad (7.2)$$

$$F_{(w,m)}^{T^4}(\tau, \bar{\tau}) \quad (7.3)$$

$$:= \frac{1}{2} \cdot \begin{cases} e^{\frac{\pi i}{2} w} \left\{ \left(\frac{\theta_3}{\eta} \right)^4 \overline{\left(\frac{\theta_3 \theta_4}{\eta^2} \right)^2} + \left(\frac{\theta_4}{\eta} \right)^4 \overline{\left(\frac{\theta_4 \theta_3}{\eta^2} \right)^2} + \left(\frac{\theta_2}{\eta} \right)^4 \overline{\left(\frac{\theta_2 \vartheta_1}{\eta^2} \right)^2} + \left(\frac{\vartheta_1}{\eta} \right)^4 \overline{\left(\frac{\vartheta_1 \theta_2}{\eta^2} \right)^2} \right\}, \\ e^{-\frac{\pi i}{2} m} \left\{ \left(\frac{\theta_3}{\eta} \right)^4 \overline{\left(\frac{\theta_3 \theta_2}{\eta^2} \right)^2} + \left(\frac{\theta_2}{\eta} \right)^4 \overline{\left(\frac{\theta_2 \theta_3}{\eta^2} \right)^2} - \left(\frac{\theta_4}{\eta} \right)^4 \overline{\left(\frac{\theta_4 \vartheta_1}{\eta^2} \right)^2} - \left(\frac{\vartheta_1}{\eta} \right)^4 \overline{\left(\frac{\vartheta_1 \theta_4}{\eta^2} \right)^2} \right\}, \\ e^{-\frac{i\pi}{2} w m} \left\{ \left(\frac{\theta_4}{\eta} \right)^4 \overline{\left(\frac{\theta_4 \theta_2}{\eta^2} \right)^2} - \left(\frac{\theta_2}{\eta} \right)^4 \overline{\left(\frac{\theta_2 \theta_4}{\eta^2} \right)^2} - \left(\frac{\theta_3}{\eta} \right)^4 \overline{\left(\frac{\theta_3 \vartheta_1}{\eta^2} \right)^2} + \left(\frac{\vartheta_1}{\eta} \right)^4 \overline{\left(\frac{\vartheta_1 \theta_3}{\eta^2} \right)^2} \right\}, \\ \left| \frac{\theta_3}{\eta} \right|^8 + \left| \frac{\theta_4}{\eta} \right|^8 + \left| \frac{\theta_2}{\eta} \right|^8 + \left| \frac{\vartheta_1}{\eta} \right|^8, \end{cases}$$

$$f_{(w,m)}(\tau) \quad (7.4)$$

$$:= \frac{1}{2} \cdot \begin{cases} e^{\frac{\pi i}{2} w} \left\{ \left(\frac{\theta_3}{\eta} \right)^2 \left(\frac{\theta_4}{\eta} \right)^2 - \left(\frac{\theta_4}{\eta} \right)^2 \left(\frac{\theta_3}{\eta} \right)^2 - \left(\frac{\theta_2}{\eta} \right)^2 \left(\frac{\vartheta_1}{\eta} \right)^2 - \left(\frac{\vartheta_1}{\eta} \right)^2 \left(\frac{\theta_2}{\eta} \right)^2 \right\}, \\ e^{-\frac{\pi i}{2} m} \left\{ \left(\frac{\theta_3}{\eta} \right)^2 \left(\frac{\theta_2}{\eta} \right)^2 - \left(\frac{\theta_2}{\eta} \right)^2 \left(\frac{\theta_3}{\eta} \right)^2 + \left(\frac{\theta_4}{\eta} \right)^2 \left(\frac{\vartheta_1}{\eta} \right)^2 + \left(\frac{\vartheta_1}{\eta} \right)^2 \left(\frac{\theta_4}{\eta} \right)^2 \right\}, \\ e^{-\frac{\pi i}{2} w m} \left\{ \left(\frac{\theta_4}{\eta} \right)^2 \left(\frac{\theta_2}{\eta} \right)^2 - \left(\frac{\theta_2}{\eta} \right)^2 \left(\frac{\theta_4}{\eta} \right)^2 + \left(\frac{\theta_3}{\eta} \right)^2 \left(\frac{\vartheta_1}{\eta} \right)^2 + \left(\frac{\vartheta_1}{\eta} \right)^2 \left(\frac{\theta_3}{\eta} \right)^2 \right\}, \\ \left(\frac{\theta_3}{\eta} \right)^4 - \left(\frac{\theta_4}{\eta} \right)^4 - \left(\frac{\theta_2}{\eta} \right)^4 - \left(\frac{\vartheta_1}{\eta} \right)^4. \end{cases}$$

The right-hand sides of (7.3) and (7.4) are listed in the order of the cases $(w \in 2\mathbb{Z}, m \in 2\mathbb{Z} + 1)$, $(w \in 2\mathbb{Z} + 1, m \in 2\mathbb{Z})$, $(w \in 2\mathbb{Z} + 1, m \in 2\mathbb{Z} + 1)$ and $(w \in 2\mathbb{Z}, m \in 2\mathbb{Z})$ from the top to the bottom. $\theta_\alpha(\tau)$ ($\alpha = 1, \dots, 4$) and $\eta(\tau)$ are the theta functions and the Dedekind η function, respectively. We have introduced $\vartheta_1(\tau) := (-i)\theta_1(\tau)$, and omitted the argument τ on the right-hand sides. For the theta functions, we follow the conventions adopted in [13].

In the above, we have explicitly written the vanishing terms involving $\theta_1 \equiv 0$, to keep track of the actual contribution from each state. We have also kept the order of the theta functions in the products for later use to identify the corresponding vertex operators. For instance, if $r < r'$, θ_α coming from the complex fermion $\psi_R^{2r} + i\psi_R^{2r+1}$ is on the left side of $\theta_{\alpha'}$ from $\psi_R^{2r'} + i\psi_R^{2r'+1}$. The order of θ_α 's in $F_{(w,m)}^{T^4}$ might not be obvious, but

can be understood from the fermionic formulation of the T_{fiber}^4 part. Under the modular transformations,

$$S: \tau \mapsto -\frac{1}{\tau}, \quad T: \tau \mapsto \tau + 1, \quad (7.5)$$

these partition functions transform covariantly as

$$\begin{aligned} Z_{(w,m)}^{\text{base}}(\tau, \bar{\tau})|_S &= Z_{(m,-w)}^{\text{base}}(\tau, \bar{\tau}), & Z_{(w,m)}^{\text{base}}(\tau, \bar{\tau})|_T &= Z_{(w,m)}^{\text{base}}(\tau, \bar{\tau}), \\ F_{(w,m)}^{T^4}(\tau, \bar{\tau})|_S &= F_{(m,-w)}^{T^4}(\tau, \bar{\tau}), & F_{(w,m)}^{T^4}(\tau, \bar{\tau})|_T &= F_{(w,w+m)}^{T^4}(\tau, \bar{\tau}), \\ f_{(w,m)}(\tau)|_S &= f_{(m,-w)}(\tau), & f_{(w,m)}(\tau)|_T &= -e^{-\frac{\pi i}{3}} f_{(w,w+m)}(\tau), \end{aligned} \quad (7.6)$$

where $f_{(w,m)}(\tau)|_T := f_{(w,m)}(\tau + 1)$, and so on.

8 Twist fields for a chiral boson

The chiral reflection $X(z) \mapsto -X(z)$ of a chiral boson X is implemented by the twist field $\Sigma(z)$ and its dual $\bar{\Sigma}(z)$ of the type in the Ashkin-Teller model, which have dimension $1/16$, and create the branch cut on the world-sheet. These twist fields have been discussed e.g. in [20–27]. The correlation functions involving these fields are, for example, given by

$$\langle \partial X(z_1) \partial X(z_2) \bar{\Sigma}(z_3) \Sigma(z_4) \rangle = -\frac{\alpha'}{2} \cdot \frac{1}{2} \frac{\sqrt{\xi} + \sqrt{\xi^{-1}}}{z_{34}^{\frac{1}{8}} z_{12}^2}, \quad (8.1)$$

$$\langle e^{ikX}(z_1) \bar{\Sigma}(z_2) \Sigma(z_3) \rangle = \frac{e^{ikx_0}}{z_{12}^{\frac{\alpha'}{4} k^2} z_{13}^{\frac{\alpha'}{4} k^2} z_{23}^{\frac{1}{8} - \frac{\alpha'}{4} k^2}}, \quad (8.2)$$

$$\langle e^{ik_1 X}(z_1) e^{ik_2 X}(z_2) \bar{\Sigma}(z_3) \Sigma(z_4) \rangle = \frac{e^{ix_0(k_1+k_2)}}{(z_{13} z_{14})^{\frac{\alpha'}{4} k_1^2} (z_{23} z_{24})^{\frac{\alpha'}{4} k_2^2} z_{34}^{\frac{1}{8} - \frac{\alpha'}{4} k_1^2 - \frac{\alpha'}{4} k_2^2}} \left(\frac{1 - \sqrt{\xi}}{1 + \sqrt{\xi}} \right)^{\frac{\alpha'}{2} k_1 k_2}, \quad (8.3)$$

where $\xi = z_{13} z_{24} / z_{23} z_{14}$, and x_0 is the zero-mode of X (see e.g. [27]). For $(z_1, z_2, z_3, z_4) = (z, w, \infty, 0)$, the correlator in (8.1) gives the two-point function in the twisted sector,

$$\langle \Sigma | \partial X(z) \partial X(w) | \Sigma \rangle = -\frac{\alpha'}{2} \cdot \frac{1}{2} \frac{\sqrt{\frac{z}{w}} + \sqrt{\frac{w}{z}}}{(z-w)^2}, \quad (8.4)$$

where $\langle \Sigma | := \lim_{z \rightarrow \infty} z^{1/8} \langle 0 | \bar{\Sigma}(z) \rangle$. For $z \rightarrow w$, this takes the same form as that in the untwisted sector $\langle \partial X(z) \partial X(w) \rangle = -\frac{\alpha'}{2} (z-w)^{-2}$.

The correlators involving e^{ikX} 's are determined by the Knizhnik-Zamolodchikov(KZ)-like equation based on the two-point function of ∂X for the twisted boundary condition (8.4), and the Sugawara-form of the energy momentum tensor, up to the zero-mode factor $e^{ix_0(\dots)}$ [25]. The derivation relies only on general properties of the twist fields and not on their details. The zero-mode factor can be fixed by a path-integral argument as in [26].

The factors such as $z_{12}^{\alpha' k^2/4}$ in (8.2) and (8.3) can be understood as coming from the self-contraction of X in e^{ikX} by adopting the same regularization as for the untwisted

boundary condition [26]. These factors ensure the correct scaling dimension of the correlators. With these remarks in mind, (8.3) with $(z_1, z_2, z_3, z_4) = (z, w, \infty, 0)$, as well as (8.4), is also understood as being obtained from the two-point function of X in the twisted sector (twisted propagator),

$$\langle \Sigma | X(z) X(w) | \Sigma \rangle = -\frac{\alpha'}{2} \log \left(\frac{\sqrt{z} - \sqrt{w}}{\sqrt{z} + \sqrt{w}} \right). \quad (8.5)$$

In the symmetric twist where both left- and right moving bosons are reflected as $X(z) + \bar{X}(\bar{z}) \rightarrow -[X(z) + \bar{X}(\bar{z})]$, the zero-mode $x_0 + \bar{x}_0$ corresponds to the location of the fixed points, which specifies a sector among the twisted sectors. Each fixed point has the corresponding twist operator [23].

We note that the momentum conservation does not need to hold in (8.2), (8.3). Since the twisted sectors should be associated with the fixed points, this may be understood also as a consequence of the break down of the translational invariance. The fixed points may supply the momenta as in the case of D-branes.

9 Formulas of integrals

The amplitudes in section 4.2 are obtained by the following formula [34, 35, 38],

$$\begin{aligned} I(\alpha, \beta; n, m) &:= \int d^2z |z|^\alpha |1-z|^\beta z^n (1-z)^m \\ &= 2\pi \frac{\Gamma(1+n+\frac{\alpha}{2})\Gamma(1+m+\frac{\beta}{2})\Gamma(-1-\frac{\alpha+\beta}{2})}{\Gamma(-\frac{\alpha}{2})\Gamma(-\frac{\beta}{2})\Gamma(2+n+m+\frac{\alpha+\beta}{2})}, \end{aligned} \quad (9.1)$$

where $\Gamma(x)$ is the Gamma function. This is rewritten in other forms by using $\Gamma(z)\Gamma(1-z) = \pi/\sin \pi z$.

In section 5.2, we need to evaluate the integral,

$$J(\alpha, \beta; \bar{\alpha}, \bar{\beta}; \bar{\gamma}) := \int d^2z z^\alpha (1-z)^\beta \bar{z}^{\bar{\alpha}} (1-\bar{z})^{\bar{\beta}} \left(\frac{1-\sqrt{\bar{z}}}{1+\sqrt{\bar{z}}} \right)^{\bar{\gamma}}. \quad (9.2)$$

The integral is first defined in the parameter region, in which the integral is convergent, and then continued to other regions as in (9.1). Because of the branch cuts, the phases/branches need to be defined appropriately. Below, we follow the standard procedure (see e.g. [35, 51]).

We set $z = u_1 + iu_2$ ($u_1, u_2 \in \mathbb{R}$). We also take $|\arg z| < \pi$, and then $\sqrt{z} = -1$ is out of the integration region. The branch points on the u_2 -plane are at $u_2 = \pm iu_1, \pm i(u_1 - 1)$. We deform the contour of u_2 along the real axis to the one along the imaginary axis by $u_2 \rightarrow ie^{-2i\epsilon}u_2 \approx i(1-2i\epsilon)u_2$ with small $\epsilon > 0$. The original z and \bar{z} become $z \rightarrow u_- + i\epsilon(u_+ - u_-)$, $\bar{z} \rightarrow u_+ - i\epsilon(u_+ - u_-)$, where $u_\pm := u_1 \pm u_2$ with $u_1, u_2 \in \mathbb{R}$. The integration measure is $\int d^2z = 2i \int du_1 du_2 = i \int du_+ du_-$.

The small imaginary part in u_- specifies the way that the contour avoids the branch points. Explicitly, it is given as in figure 2 according to the value of u_+ , namely, $u_+ < 0$, $0 < u_+ < 1$ or $1 < u_+$. As long as the integral is convergent, the contributions from

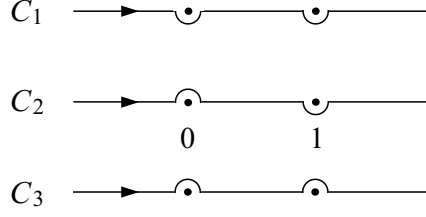


Figure 2. Contours of u_- -integral. C_1, C_2, C_3 are for $u_+ < 0, 0 < u_+ < 1$ and $1 < u_+$, respectively.

$u_+ < 0$ and $1 < u_+$ vanish, which is confirmed by closing the contour in the lower/upper half plane. Thus, we are left with

$$J \sim i \int_0^1 du_+ u_+^{\bar{\alpha}} (1 - u_+)^{\bar{\beta}} \left(\frac{1 - \sqrt{u_+}}{1 + \sqrt{u_+}} \right)^{\bar{\gamma}} \times \int_{C_2} du_- u_-^{\alpha} (1 - u_-)^{\beta}, \quad (9.3)$$

where C_2 is the second contour in figure 2. We define the phase of the integrand for $u_- < 0$ by 1 for $u_+ < 0$, $e^{\pi i \bar{\alpha}}$ for $0 < u_+ < 1$ and $e^{\pi i (\bar{\alpha} + \bar{\beta})}$ for $1 < u_+$. 1, $e^{\pi i \bar{\alpha}}$, $e^{\pi i (\bar{\alpha} + \bar{\beta})}$ are understood as the relative phases coming from the integrand for u_+ . This choice/definition corresponds to choosing the phase so that it becomes 1 when $\alpha = \bar{\alpha}$, $\beta = \bar{\beta}$ and u_{\pm} are in the same interval of $(-\infty, 0)$, $(0, 1)$ or $(1, \infty)$. We also define $\sqrt{u_+}$ without a phase/sign for $u_+ > 0$.

By deforming the contour C_2 for u_- to be wrapped around $u_- = 1$, we arrive at

$$J = -2e^{\pi i (\bar{\alpha} - \alpha)} \sin(\pi \beta) \times J_L \times J_R, \quad (9.4)$$

where

$$\begin{aligned} J_L &= \int_1^{\infty} du_- |u_-|^{\alpha} |u_- - 1|^{\beta} = B(1 + \beta, -\alpha - \beta - 1), \\ J_R &= \int_0^1 du_+ |u_+|^{\bar{\alpha}} |1 - u_+|^{\bar{\beta}} \left(\frac{1 - \sqrt{|u_+|}}{1 + \sqrt{|u_+|}} \right)^{\bar{\gamma}}, \end{aligned} \quad (9.5)$$

and $B(a, b)$ is the beta function. J_R is then evaluated by making a change of variables $\sqrt{u_+} = v$,

$$\begin{aligned} J_R(\bar{\alpha}, \bar{\beta}, \bar{\gamma}) &= 2 \int_0^1 dv v^{1+2\bar{\alpha}} (1 - v)^{\bar{\beta} + \bar{\gamma}} (1 + v)^{\bar{\beta} - \bar{\gamma}} \\ &= 2B(2 + 2\bar{\alpha}, 1 + \bar{\beta} + \bar{\gamma}) F(2 + 2\bar{\alpha}, \bar{\gamma} - \bar{\beta}; 3 + 2\bar{\alpha} + \bar{\beta} + \bar{\gamma}; -1), \end{aligned} \quad (9.6)$$

where $F(a, b, c; z)$ is the hypergeometric function. The possible poles of J_R come from the factor $\Gamma(2 + 2\bar{\alpha})\Gamma(1 + \bar{\beta} + \bar{\gamma})$ in the beta function, since $\frac{1}{\Gamma(c)}F(a, b, c; z)$ is an entire function of a, b, c for fixed z with $|z| < 1$ or $\text{Re } z < 1/2$ [52]. They can be cancelled with the zeros from the other part. Combining (9.5) and (9.6), we obtain

$$J(\alpha, \beta; \bar{\alpha}, \bar{\beta}; \bar{\gamma}) = 2\pi e^{\pi i (\bar{\alpha} - \alpha)} \frac{\Gamma(-1 - \alpha - \beta)}{\Gamma(-\alpha)\Gamma(-\beta)} J_R(\bar{\alpha}, \bar{\beta}, \bar{\gamma}). \quad (9.7)$$

When $\bar{\gamma} = 0$, by using the formulas,

$$F(a, b; a - b + 1; -1) = \frac{2^{-a} \sqrt{\pi} \Gamma(a - b + 1)}{\Gamma\left(\frac{a+1}{2}\right) \Gamma\left(\frac{a}{2} - b + 1\right)}, \quad \Gamma(2z) = \frac{2^{2z-1}}{\sqrt{\pi}} \Gamma(z) \Gamma\left(z + \frac{1}{2}\right), \quad (9.8)$$

one finds that

$$J_R(\bar{\alpha}, \bar{\beta}, 0) = \frac{\Gamma(1 + \bar{\alpha}) \Gamma(1 + \bar{\beta})}{\Gamma(2 + \bar{\alpha} + \bar{\beta})}, \quad (9.9)$$

and thus

$$J(\alpha, \beta; \bar{\alpha}, \bar{\beta}; 0) = 2\pi e^{\pi i(\bar{\alpha} - \alpha)} \frac{\Gamma(-1 - \alpha - \beta) \Gamma(1 + \bar{\alpha}) \Gamma(1 + \bar{\beta})}{\Gamma(-\alpha) \Gamma(-\beta) \Gamma(2 + \bar{\alpha} + \bar{\beta})}. \quad (9.10)$$

By setting

$$\bar{\gamma} = 0, \quad \alpha \rightarrow \frac{\alpha}{2}, \quad \beta \rightarrow \frac{\beta}{2}, \quad \bar{\alpha} \rightarrow \frac{\alpha}{2} + n, \quad \bar{\beta} \rightarrow \frac{\beta}{2} + m, \quad (9.11)$$

(9.10) is reduced to (9.1) up to a phase $e^{\pi i(\bar{\alpha} - \alpha)}$ due to the difference of the conventions of the phase. In the main text, we drop this phase to conform to (9.1) and the definition of the phase of \sqrt{z} in the computation of the correlators.

The integral with the factor from the twisted propagator also in the left-mover,

$$\mathcal{J} := \int d^2z z^\alpha (1-z)^\beta \bar{z}^{\bar{\alpha}} (1-\bar{z})^{\bar{\beta}} \left(\frac{1-\sqrt{z}}{1+\sqrt{z}}\right)^\gamma \left(\frac{1-\sqrt{\bar{z}}}{1+\sqrt{\bar{z}}}\right)^{\bar{\gamma}}, \quad (9.12)$$

is evaluated similarly. In that case, the beta function for J_L in (9.5) is replaced by a hypergeometric function as

$$\begin{aligned} \mathcal{J}(\alpha, \beta; \bar{\alpha}, \bar{\beta}; \gamma; \bar{\gamma}) &= -2e^{\pi i(\bar{\alpha} - \alpha)} \sin(\pi\beta) \times \mathcal{J}_L(\alpha, \beta, \gamma) \times J_R(\bar{\alpha}, \bar{\beta}, \bar{\gamma}), \\ \mathcal{J}_L(\alpha, \beta, \gamma) &= J_R(-\alpha - \beta - 2, \beta, \gamma). \end{aligned} \quad (9.13)$$

Compared with (9.6) for the right-mover, \mathcal{J}_L has the argument $-\alpha - \beta - 2$ instead of α (up to the overline ($\bar{\quad}$)), which implies that the roles of the t - and u -channels are exchanged.

We also list the formulas of the hypergeometric function used in the main text [52],

$$F(a, b; c; z) = (1-z)^{-a} F\left(a, c-b; c; \frac{z}{z-1}\right), \quad (9.14)$$

$$F\left(a, 1-a; c; \frac{1}{2}\right) = \frac{2^{1-c} \sqrt{\pi} \Gamma(c)}{\Gamma\left(\frac{c+a}{2}\right) \Gamma\left(\frac{c-a+1}{2}\right)}, \quad (9.15)$$

$$F(0, b; c; z) = 1, \quad (9.16)$$

$$F(a, b; a; z) = (1-z)^{-b}. \quad (9.17)$$

The forth formula is obtained by combining the first and the third.

10 SO(4) gamma matrices

We summarize our conventions of the SO(4) gamma matrices used in section 5.2. We denote by $|\epsilon_1, \epsilon_2\rangle$ with $\epsilon_1, \epsilon_2 = \pm$ the state corresponding to the bosonized spinor $e^{\frac{i}{2}(\epsilon_1 H^1 + \epsilon_2 H^2)}$ as in (2.9). We also set $|1\rangle = |+, +\rangle$, $|2\rangle = |-, -\rangle$, $|\dot{1}\rangle = |+, -\rangle$, $|\dot{2}\rangle = |-, +\rangle$. Then, we represent the SO(4) gamma matrices satisfying $\{\Gamma^a, \Gamma^b\} = 2\delta^{ab}$ by

$$\Gamma^1 = \sigma_1 \otimes \sigma_1, \quad \Gamma^2 = \sigma_1 \otimes \sigma_2, \quad \Gamma^3 = \sigma_1 \otimes \sigma_3, \quad \Gamma^4 = \sigma_2 \otimes \mathbf{1}, \quad (10.1)$$

where σ_j are the Pauli matrices and $\mathbf{1}$ is the 2×2 identity matrix. $\Gamma^{j\pm} := (\Gamma^{2j-1} \pm i\Gamma^{2j})/2$ ($j = 1, 2$) raise or lower ϵ_j . The basis of the states is ordered as $|1\rangle, |2\rangle, |\dot{1}\rangle, |\dot{2}\rangle$. The chirality matrix is $\Gamma_5 = i^2 \Gamma^1 \Gamma^2 \Gamma^3 \Gamma^4 = \sigma_3 \otimes \mathbf{1}$, whereas the charge conjugation matrix is $C := \Gamma^3 \Gamma^1 = \mathbf{1} \otimes i\sigma_2$, which satisfies $C^2 = -1$ and $C\Gamma^a C^{-1} = -(\Gamma^a)^T$. We also use the chiral blocks of Γ^a , C and $\Gamma^{ab} := (\Gamma^a \Gamma^b - \Gamma^b \Gamma^a)/2$ as in

$$\Gamma^a = \begin{pmatrix} 0 & (\gamma^a)_\alpha^{\dot{\beta}} \\ (\bar{\gamma}^a)_{\dot{\alpha}}^\beta & 0 \end{pmatrix}, \quad C = \begin{pmatrix} \mathcal{C}^{\alpha\beta} & 0 \\ 0 & \bar{\mathcal{C}}^{\dot{\alpha}\dot{\beta}} \end{pmatrix}, \quad \Gamma^{ab} = \begin{pmatrix} (\gamma^{ab})_\alpha^\beta & 0 \\ 0 & (\bar{\gamma}^{ab})_{\dot{\alpha}}^{\dot{\beta}} \end{pmatrix}. \quad (10.2)$$

In particular, $\mathcal{C}^{\alpha\beta} = (i\sigma_2)^{\alpha\beta}$. The indices are raised and lowered by C and C^{-1} , respectively.

Open Access. This article is distributed under the terms of the Creative Commons Attribution License ([CC-BY 4.0](https://creativecommons.org/licenses/by/4.0/)), which permits any use, distribution and reproduction in any medium, provided the original author(s) and source are credited.

References

- [1] S. Hellerman, J. McGreevy and B. Williams, *Geometric constructions of nongeometric string theories*, *JHEP* **01** (2004) 024 [[hep-th/0208174](#)] [[INSPIRE](#)].
- [2] A. Dabholkar and C. Hull, *Duality twists, orbifolds, and fluxes*, *JHEP* **09** (2003) 054 [[hep-th/0210209](#)] [[INSPIRE](#)].
- [3] A. Flournoy, B. Wecht and B. Williams, *Constructing nongeometric vacua in string theory*, *Nucl. Phys. B* **706** (2005) 127 [[hep-th/0404217](#)] [[INSPIRE](#)].
- [4] C.M. Hull, *A Geometry for non-geometric string backgrounds*, *JHEP* **10** (2005) 065 [[hep-th/0406102](#)] [[INSPIRE](#)].
- [5] C. Hull and B. Zwiebach, *Double Field Theory*, *JHEP* **09** (2009) 099 [[arXiv:0904.4664](#)] [[INSPIRE](#)].
- [6] C.M. Hull, *Doubled Geometry and T-Folds*, *JHEP* **07** (2007) 080 [[hep-th/0605149](#)] [[INSPIRE](#)].
- [7] D.S. Berman and D.C. Thompson, *Duality Symmetric String and M-theory*, *Phys. Rept.* **566** (2014) 1 [[arXiv:1306.2643](#)] [[INSPIRE](#)].
- [8] E. Plauschinn, *Non-geometric backgrounds in string theory*, *Phys. Rept.* **798** (2019) 1 [[arXiv:1811.11203](#)] [[INSPIRE](#)].
- [9] K. Aoki, E. D'Hoker and D.H. Phong, *On the construction of asymmetric orbifold models*, *Nucl. Phys. B* **695** (2004) 132 [[hep-th/0402134](#)] [[INSPIRE](#)].

- [10] A. Flournoy and B. Williams, *Nongeometry, duality twists, and the worldsheet*, *JHEP* **01** (2006) 166 [[hep-th/0511126](#)] [[INSPIRE](#)].
- [11] S. Hellerman and J. Walcher, *Worldsheet CFTs for Flat Monodromies*, [hep-th/0604191](#) [[INSPIRE](#)].
- [12] S. Kawai and Y. Sugawara, *D-branes in T-fold conformal field theory*, *JHEP* **02** (2008) 027 [[arXiv:0709.0257](#)] [[INSPIRE](#)].
- [13] Y. Satoh, Y. Sugawara and T. Wada, *Non-supersymmetric Asymmetric Orbifolds with Vanishing Cosmological Constant*, *JHEP* **02** (2016) 184 [[arXiv:1512.05155](#)] [[INSPIRE](#)].
- [14] Y. Satoh and Y. Sugawara, *Lie algebra lattices and strings on T-folds*, *JHEP* **02** (2017) 024 [[arXiv:1611.08076](#)] [[INSPIRE](#)].
- [15] J.A. Harvey and G.W. Moore, *An Uplifting Discussion of T-duality*, *JHEP* **05** (2018) 145 [[arXiv:1707.08888](#)] [[INSPIRE](#)].
- [16] Y. Sugawara and T. Wada, *More on Non-supersymmetric Asymmetric Orbifolds with Vanishing Cosmological Constant*, *JHEP* **08** (2016) 028 [[arXiv:1605.07021](#)] [[INSPIRE](#)].
- [17] K. Aoyama and Y. Sugawara, *non-SUSY Gepner Models with Vanishing Cosmological Constant*, *PTEP* **2020** (2020) 103B01 [[arXiv:2005.13198](#)] [[INSPIRE](#)].
- [18] K. Aoyama and Y. Sugawara, *non-SUSY Heterotic String Vacua of Gepner Models with Vanishing Cosmological Constant*, *PTEP* **2021** (2021) 033B03 [[arXiv:2102.00683](#)] [[INSPIRE](#)].
- [19] Y. Satoh and Y. Sugawara, *Notes on Vanishing Cosmological Constant without Bose-Fermi Cancellation*, *PTEP* **2022** (2022) 053B04 [[arXiv:2111.09663](#)] [[INSPIRE](#)].
- [20] M. Bershadsky, *On Off-shell States in Bosonic String Theory*, *Int. J. Mod. Phys. A* **1** (1986) 443 [[INSPIRE](#)].
- [21] L.J. Dixon, D. Friedan, E.J. Martinec and S.H. Shenker, *The Conformal Field Theory of Orbifolds*, *Nucl. Phys. B* **282** (1987) 13 [[INSPIRE](#)].
- [22] A.B. Zamolodchikov, *Conformal Scalar Field on the Hyperelliptic Curve and Critical Ashkin-teller Multipoint Correlation Functions*, *Nucl. Phys. B* **285** (1987) 481 [[INSPIRE](#)].
- [23] P.H. Ginsparg, *Apled Conformal Field Theory*, in *Les Houches Summer School in Theoretical Physics: Fields, Strings, Critical Phenomena*, (1988) [[hep-th/9108028](#)] [[INSPIRE](#)].
- [24] A. Hashimoto, *Dynamics of Dirichlet-Neumann open strings on D-branes*, *Nucl. Phys. B* **496** (1997) 243 [[hep-th/9608127](#)] [[INSPIRE](#)].
- [25] J. Fröhlich, O. Grandjean, A. Recknagel and V. Schomerus, *Fundamental strings in $D_p - D_q$ brane systems*, *Nucl. Phys. B* **583** (2000) 381 [[hep-th/9912079](#)] [[INSPIRE](#)].
- [26] P. Mukhopadhyay, *Oscillator representation of the BCFT construction of D-branes in vacuum string field theory*, *JHEP* **12** (2001) 025 [[hep-th/0110136](#)] [[INSPIRE](#)].
- [27] L. Mattiello and I. Sachs, \mathbb{Z}_2 boundary twist fields and the moduli space of D-branes, *JHEP* **07** (2018) 099 [[arXiv:1803.07500](#)] [[INSPIRE](#)].
- [28] S. Hamidi and C. Vafa, *Interactions on Orbifolds*, *Nucl. Phys. B* **279** (1987) 465 [[INSPIRE](#)].
- [29] A. Giveon, M. Porrati and E. Rabinovici, *Target space duality in string theory*, *Phys. Rept.* **244** (1994) 77 [[hep-th/9401139](#)] [[INSPIRE](#)].

- [30] A. Dabholkar and C. Hull, *Generalised T-duality and non-geometric backgrounds*, *JHEP* **05** (2006) 009 [[hep-th/0512005](#)] [[INSPIRE](#)].
- [31] C. Condeescu, I. Florakis, C. Kounnas and D. Lüüst, *Gauged supergravities and non-geometric Q/R-fluxes from asymmetric orbifold CFT's*, *JHEP* **10** (2013) 057 [[arXiv:1307.0999](#)] [[INSPIRE](#)].
- [32] K. Itoh, M. Kato, H. Kunitomo and M. Sakamoto, *Vertex Construction and Zero Modes of Twisted Strings on Orbifolds*, *Nucl. Phys. B* **306** (1988) 362 [[INSPIRE](#)].
- [33] M.B. Green, J.H. Schwarz and E. Witten, *Superstring theory. Vol. 1: Introduction*, Cambridge University Press, Cambridge, U.K. (1987) [[INSPIRE](#)].
- [34] R. Blumenhagen, D. Lüüst and S. Theisen, *Basic concepts of string theory*, Springer, Berlin, Germany (2013) [[DOI](#)].
- [35] H. Kawai, D.C. Lewellen and S.H.H. Tye, *A Relation Between Tree Amplitudes of Closed and Open Strings*, *Nucl. Phys. B* **269** (1986) 1 [[INSPIRE](#)].
- [36] D.J. Gross and P.F. Mende, *String Theory Beyond the Planck Scale*, *Nucl. Phys. B* **303** (1988) 407 [[INSPIRE](#)].
- [37] V.A. Kostelecky, O. Lechtenfeld, W. Lerche, S. Samuel and S. Watamura, *Conformal Techniques, Bosonization and Tree Level String Amplitudes*, *Nucl. Phys. B* **288** (1987) 173 [[INSPIRE](#)].
- [38] J. Polchinski, *String theory. Vol. 1: An introduction to the bosonic string*, Cambridge University Press, Cambridge, U.K. (1998) [[DOI](#)].
- [39] J. Erler, D. Jungnickel, J. Lauer and J. Mas, *String emission from twisted sectors: cocycle operators and modular background symmetries*, *Annals Phys.* **217** (1992) 318 [[INSPIRE](#)].
- [40] O. Hohm and B. Zwiebach, *Double field theory at order α'* , *JHEP* **11** (2014) 075 [[arXiv:1407.3803](#)] [[INSPIRE](#)].
- [41] G. Aldazabal, D. Marques and C. Núñez, *Double Field Theory: A Pedagogical Review*, *Class. Quant. Grav.* **30** (2013) 163001 [[arXiv:1305.1907](#)] [[INSPIRE](#)].
- [42] E. Wong and I. Affleck, *Tunneling in quantum wires: A Boundary conformal field theory approach*, *Nucl. Phys. B* **417** (1994) 403 [[cond-mat/9311040](#)] [[INSPIRE](#)].
- [43] V.B. Petkova and J.B. Zuber, *Generalized twisted partition functions*, *Phys. Lett. B* **504** (2001) 157 [[hep-th/0011021](#)] [[INSPIRE](#)].
- [44] C. Bachas, J. de Boer, R. Dijkgraaf and H. Ooguri, *Permeable conformal walls and holography*, *JHEP* **06** (2002) 027 [[hep-th/0111210](#)] [[INSPIRE](#)].
- [45] C. Bachas and I. Brunner, *Fusion of conformal interfaces*, *JHEP* **02** (2008) 085 [[arXiv:0712.0076](#)] [[INSPIRE](#)].
- [46] Y. Satoh, *On supersymmetric interfaces for string theory*, *JHEP* **03** (2012) 072 [[arXiv:1112.5935](#)] [[INSPIRE](#)].
- [47] C. Bachas, I. Brunner and D. Roggenkamp, *A worldsheet extension of $O(d, d : Z)$* , *JHEP* **10** (2012) 039 [[arXiv:1205.4647](#)] [[INSPIRE](#)].
- [48] S. Elitzur, B. Karni, E. Rabinovici and G. Sarkissian, *Defects, Super-Poincaré line bundle and Fermionic T-duality*, *JHEP* **04** (2013) 088 [[arXiv:1301.6639](#)] [[INSPIRE](#)].

- [49] Y. Satoh and Y. Sugawara, *Non-geometric Backgrounds Based on Topological Interfaces*, *JHEP* **07** (2015) 022 [[arXiv:1502.05776](#)] [[INSPIRE](#)].
- [50] T. Kojita, C. Maccaferri, T. Masuda and M. Schnabl, *Topological defects in open string field theory*, *JHEP* **04** (2018) 057 [[arXiv:1612.01997](#)] [[INSPIRE](#)].
- [51] V.S. Dotsenko, *Lectures on conformal field theory*, *Adv. Stud. Pure Math.* **16** (1988).
- [52] H. Batemanm *Higher transcendental functions. Vol. 1*, McGraw-Hill Book Company, New York, U.S.A. (1953).